



Formulation of a dry powder for inhalation combining ciclesonide and indacaterol maleate using spray drying

Laure-Anne Bya^a, Benedetta Bottero^b, Alice Coeurderoi^a, Tuan Nghia Dinh^a,
Pierre-Yves Sacré^c, Eric Ziemons^d, Didier Cataldo^b, Géraldine Piel^a, Brigitte Evrard^a,
Anna Lechanteur^{a,*}

^a University of Liege, Laboratory of Pharmaceutical Technology and Biopharmacy, Center for Interdisciplinary Research on Medicines (CIRM), Avenue Hippocrate 15, 4000 Liege, Belgium

^b University of Liege, Laboratory of Tumor and Development Biology, GIGA-Cancer, Avenue Hippocrate 15, 4000 Liege, Belgium

^c University of Liege, CIRM, Research Support Unit in Chemometrics, Department of Pharmacy, Avenue Hippocrate 15, 4000 Liege, Belgium

^d University of Liege, CIRM, ViBra-Sante HUB, Laboratory of Pharmaceutical Analytical Chemistry, Department of Pharmacy, Avenue Hippocrate 15, 4000 Liege, Belgium

ARTICLE INFO

Keywords:

Dry powder
Spray drying
Powder engineering
Cyclodextrin complexation
PreciseInhale®

ABSTRACT

Dry powders for inhalation are evolving to address the challenge of maximizing lung deposition, with growing interest in carrier-free formulations shaping future therapies. This study focuses on developing an inhalation powder with optimal properties, combining ciclesonide and indacaterol, a combination treatment for asthma not yet available on the market. Using spray-drying technology with cyclodextrins, ultra-flying microparticles aim to be produced to enhance aerosolization and therapeutic efficacy. Cyclodextrin screening identified Crystmab as the most effective for ciclesonide complexation, enabling stable solution atomization, while HPβCD was selected to create deflated particle shapes in a spray-dried suspension.

The impact of active pharmaceutical ingredient solubilization state and solid content on powder properties was investigated, revealing that the solutions provided a more suitable particle size distribution for inhalation. Moreover, the atomized solutions led to fine particle fractions exceeding 60 % for both drugs, outperforming commercial products due to this enhanced distribution. Aerodynamic performance was further assessed under reduced flow rates using the Next Generation Impactor, showing no significant reduction in lung deposition at 60 L/min for atomized solutions. The optimized powders also demonstrated higher lung deposition of indacaterol maleate compared to Onbrez®, with findings confirmed using the PreciseInhale® system, providing comprehensive insights into aerosolization behavior. These results highlight the importance of advancing *in vitro* methods to better predict *in vivo* performance and support the development of more effective inhaled therapies.

Overall, this work presents a stable, carrier-free inhalation powder with a novel drug combination that achieves efficient lung deposition and six-month stability.

1. Introduction

Asthma and chronic obstructive pulmonary disease (COPD)

represent the foremost chronic inflammatory disorders of the airways, commonly treated via inhaled drug administration (Barnes, 2017; Cataldo et al., 2017). Inhalation ensures targeted delivery, rapid

Abbreviations: API, Active Pharmaceutical Ingredient; CI, Cascade Impactor; CIC, Ciclesonide; COPD, Chronic Obstructive Pulmonary Disease; Dae, Aerodynamic Diameter; DepthD, Depth of dimples; DPI, Dry Powder Inhaler; ED, Emitted Dose; FPD, Fine Particle Dose; FPF, Fine Particle Fraction; GSD, Geometric Standard Deviation; HPβCD, Hydroxypropyl-β-Cyclodextrin; HPLC, High Performance Liquid Chromatography; ICS, Inhaled Corticosteroid; ICH, International Council for Harmonisation of Technical Requirements for Pharmaceuticals for Human Use; IND, Indacaterol Maleate; LABA, Long-Acting Beta Agonist; MMAD, Mass Median Aerodynamic Diameter; ND, Number dimples; NGI, Next Generation Impactor; PE, Péclet Number; pMDI, Pressurized Metered-Dose Inhaler; PSD, Particle Size Distribution; RD, Recovery Dose; RH, Relative Humidity; RSD, Relative Standard Deviation; SD, Spray-Drying; SEM, Scanning Electron Microscopy; SMI, Soft-Mist Inhaler; TGA, Thermogravimetric Analysis.

* Corresponding author.

E-mail address: anna.lechanteur@uliege.be (A. Lechanteur).

<https://doi.org/10.1016/j.ijpharm.2025.125696>

Received 12 February 2025; Received in revised form 24 April 2025; Accepted 6 May 2025

Available online 7 May 2025

0378-5173/© 2025 Elsevier B.V. All rights are reserved, including those for text and data mining, AI training, and similar technologies.

therapeutic onset, and minimal side effects, using devices like nebulizers, metered-dose inhalers (pMDIs), soft-mist inhalers (SMIs), and dry powder inhalers (DPIs) (Lechanteur and Evrard, 2020; Myers, 2013; Wang et al., 2024). Among them, DPIs stand out due to their lack of propellant gases and the absence of coordination between inhalation and actuation. Most notably, their dry formulation enhances drug stability, making DPIs ideal for delivering sensitive molecules like biopharmaceuticals, a promising advancement in pulmonary drug delivery (Chang and Chan, 2022; Marante et al., 2020; Shahin and Chablani, 2023). Beyond the benefits, the main interest in developing DPIs lies in the ability to improve dry powders through particle engineering, ultimately optimizing their performances (Scherließ et al., 2022).

Indeed, in the field of DPI, treatment efficacy relies not only on the inhalation device but on specific physicochemical properties of powders that facilitate deep lung deposition (Negi et al., 2023). Factors such as the powder's crystalline or amorphous nature, surface charges, residual moisture, and particle morphology significantly impact solubility, stability, and pulmonary deposition (Chaurasiya and Zhao, 2021; Spahn et al., 2022). Among the various criteria of powders, the most critical is their aerodynamic diameter (D_{ae}), ideally ranging between 1 and 5 µm, ensuring effective lung deposition and minimizing upper airway impaction (Darquenne, 2020; Magramane et al., 2023; Zillen et al., 2021). However, small particle size increases cohesive forces, affecting powder flow and complicating DPI manufacturing (Karner and Anne Urbanetz, 2011; Spahn et al., 2022). To address this, the most widely used technique in current inhalation powder development involves adsorbing micronized active pharmaceutical ingredients (API) onto a sugar-based carrier, typically monohydrated lactose (Hebbink et al., 2022; L. Wu et al., 2014). Yet, excessive carrier-API interactions and coarse particle impaction contribute to inefficient delivery, with less than one-third of the medication reaching the deep lung (de Boer et al., 2017; Lechanteur and Evrard, 2020).

Multiple approaches can be employed to enhance lung deposition, either separately or in combination. These include the optimization of inhalation devices, the refinement of carrier properties, the development of optimized micronized carrier-free powders (Elsayed et al., 2024; Shahin and Chablani, 2023). As part of these tactics, carrier-free powders development has gained lots of attention in recent years, with techniques like self-agglomeration through granulation or spheronization, as seen in Pulmicort® Turbuhaler® before its market withdrawal in 2021 (Sun, 2016). Additionally, spray-drying (SD) technology has been pivotal in optimizing carrier-free powders properties, transforming concentrated liquid feedstocks into dry particles through atomization in a heated gas stream (Sollohub and Cal, 2010; Sosnik and Seremeta, 2015). This method is cost-effective, adaptable, and reproducible, allowing the creation of engineered DPIs with controlled properties (Ziaee et al., 2019). Modifying parameters like temperature, nozzle pressure, and solid content, especially with carbohydrate matrices, enables the development of unique formulations like PulmoSphere™ and PulmoSol™ (Weers and Tarara, 2014). This technology employs an emulsion-based SD process to create lightweight, spherical particles, characterized by a high porosity, that reduce surface contact and agglomeration, enhancing flow, dispersion, and intrapulmonary deposition (Geller et al., 2011; Mitta et al., 2024; Weers and Tarara, 2014). Furthermore, spherical deflated particles appear to be a very interesting alternative, particularly in terms of increased lung deposition. Dufour et al. (Dufour et al., 2015) successfully developed spherical deflated particles by atomizing hydroxypropyl-β-cyclodextrin (HPβCD) with budesonide. Lechanteur et al. (Lechanteur et al., 2023) identified optimal drying parameters that leveraged this excipient to create a DPI combining budesonide and formoterol, ultimately enhancing lung deposition profile due to this specific morphology. Indeed, deflated particles, characterized by lower density, optimized particle size, and irregular surfaces that reduce cohesion forces, have demonstrated superior *in vitro* lung deposition compared to traditional lactose-based formulations, thereby significantly enhancing pulmonary delivery

efficiency. Gresse et al. have recently demonstrated the need to optimize the flow properties of these micronized powders to support industrial-scale production. The blend of coarse-carrier with such spray-dried micronized powder promote accurate capsules filling (Gresse et al., 2024). These examples underscore the critical but challenging role of particle engineering, where fine-tuning parameters and precise excipient selection can impact multiple properties, requiring careful balance to achieve optimal results (Scherließ et al., 2022).

This study aimed to develop an optimized DPI featuring an innovative combination of two anti-asthmatic agents, ciclesonide, an inhaled corticosteroid (ICS), and indacaterol maleate, a long-acting beta agonist (LABA), using spray-drying technology. IND, categorized as an “ultra-LABA” provides rapid bronchodilation within 5 min, lasting up to 24 h (Rossi and Polese, 2013). Its once-daily dosing enhances patient adherence and quality of life by combining convenience with sustained therapeutic efficacy. Due to exacerbation risks associated with monotherapy, IND is combined with CIC, an ICS with established therapeutic efficacy but unavailable in DPIs formulation and currently only available as a monotherapy (Alvesco®) (Deeks et al., 2008; Rodrigo and Castro-Rodríguez, 2012). Furthermore, CIC is a prodrug that, following intracellular uptake within bronchial epithelial cells, is converted into its active metabolite, desisobutyl-β-ciclesonide (des-CIC). This targeted activation profile not only enhances its therapeutic efficacy but also contributes to minimizing both local adverse effects and systemic side effects, offering a favorable safety profile within inhaled corticosteroid therapies (Nave and McCracken, 2008). This combination could enhance the synergistic therapeutic benefits for asthma and COPD treatment, offering the convenience of a similar posology with a once-daily administration, while benefiting from the advantages of optimized DPIs developed by the SD technology.

The drying outcomes of solution and suspension atomization on the properties of the final developed powders were examined, along with the influence of variations in solid content. Given the high hydrophobicity of CIC and prior research highlighting the advantages of a deflated morphology combined with a promising safety profile for inhalation, cyclodextrins are incorporated to enhance the solubility of the corticosteroid, allowing the atomization of a solution and the comparison to a suspension (Evrard et al., 2004; Lechanteur et al., 2023, 2022; Matilainen et al., 2008). Furthermore, the *in vitro* aerodynamic performance of both DPIs was assessed using the Next Generation Impactor (NGI), while the PreciseInhale® system was employed to evaluate aerosolization performance and provide insights into powder dispersibility. Analysis of the trends observed between these two techniques allowed for a better understanding and optimization of dry powder inhalers performance. Overall, this work aimed to develop an innovative DPI formulation that combines a novel API pairing with the creation of spherical, deflated particles to optimize inhalation properties and enhance lung deposition, thereby addressing a gap in current market options.

2. Materials and methods

2.1. Materials

Micronized ciclesonide (CIC) was kindly provided from NewChem spa (Milano, Italy) and indacaterol maleate (IND) was obtained from LEAP Chem CO (Wan Chai, Hong Kong). Hydroxypropyl-β-cyclodextrin (HPβCD), Crysmeb® (a methylated βCD) and hydroxypropyl-γ-cyclodextrin (HPγCD) were kindly provided by Roquette (Lestrem, France).

HPLC-grade methanol and absolute ethanol were acquired from J.T. Baker (Deventer, The Netherlands) and ThermoFisher Scientific (Geel, Belgium), respectively. Ammonium acetate and 25 % ammonia solution were sourced from Sigma-Aldrich (St. Louis, MO, USA). Water was purified using a Millipore system (18.2 MΩ/cm resistivity, Milli-Q) and subsequently filtered through a 0.22 µm Millipore Millipak® 40 disposable filter units (Millipore Corporation, USA).

Hydroxypropyl methylcellulose capsules, size 3 and suitable for inhalation, were provided by Capsugel® (Lonza, Colmar, France) and used with the Onbrez® Breezhaler® (Novartis Pharma BV, Basel, Switzerland), a low-resistance device with a resistance of $0.0177 \text{ (kPa)}^{0.5} \text{ (min L}^{-1}\text{)}$ (Abadelah et al., 2018; Dal Negro, 2015).

2.2. Indacaterol maleate and ciclesonide quantification

The quantification of CIC and IND was conducted using an Agilent 1100 Series HPLC system (Santa Clara, USA). The analysis employed a $3 \times 50 \text{ mm}$ column packed with $3.5 \mu\text{m}$ C18 material (X Bridge BEH C18 Column) in conjunction with a VanGuard Cartridge pre-column, 3/PK. Detection was carried out with a UV detector set to 243 nm. The mobile phase comprised an ammonium acetate buffer at pH 10 and methanol, with the following gradient elution program: 0 min – 80/20 (v/v); 1 min – 80/20 (v/v); 10 min – 5/95 (v/v); 13 min – 5/95 (v/v); 13.5 min – 80/20 (v/v); 20 min – 80/20 (v/v). The flow rate was maintained at 0.7 mL/min, and the column temperature was set to 30°C , while the sampler temperature was maintained at 10°C .

2.3. Determination of the degradation temperature of raw CIC and IND

Thermogravimetric Analysis (TGA) was conducted using a Mettler-Toledo instrument (Schwerzenbach, Switzerland) to assess the degradation temperature of CIC and IND raw material. The analysis involved 5 mg of API placed in aluminum pans, with a heating rate of 20°C/min ,

$$\text{Drying process yield (\%)} = \frac{\text{Amount of powder collected after atomization (g)}}{\text{Total amount of powder implemented in the atomized liquid (g)}} \cdot 100 \quad (1)$$

ranging from 25 to 500°C , under a nitrogen flow of 20 mL/min.

2.4. Phase solubility diagram

The complexation of CIC with cyclodextrins was investigated using the phase solubility diagram method as described by Higuchi and Connors (Saokham et al., 2018). CIC was added in excess to 4.0 mL of purified water containing increasing concentrations of cyclodextrins ranging from 0 to 200 mM. The vials were then placed in a shaker bath at 37°C and 150 RPM for 48 h where CIC excess was maintained until equilibrium was reached. Afterward, the samples were filtered through a $0.22 \mu\text{m}$ pore filter, transferred to vials, and absolute ethanol was added to prevent any potential APIs precipitation. The vials were subsequently analyzed using HPLC, as described in Section 2.2.

2.5. Feedstocks preparation

Each prepared liquid formulation containing the two active ingredients of interest was prepared exclusively using purified water, with a total volume of 100.0 mL. The formulations had a solid content of either 5 or 10 % (w/v), representing the proportion of solid substances in the atomized liquid. As mentioned in the introduction, due to high hydrophobicity of CIC, formulation and atomization of a solution (SOL_{Crysmeb}) and a suspension (SUS_{HPβCD}) were investigated. The suspension included HPβCD and a surfactant agent (Tween® 80). Solubilization efficiency was enhanced with Crysmeb, a methyl-β-cyclodextrin, as determined by phase-solubility tests described in Section 2.4. For the preparation of the solutions, once Crysmeb was fully dissolved, CIC was added and allowed to fully complex with the cyclodextrin. IND was subsequently introduced and mixed until complete dissolution. For the formulation of the suspensions, HPβCD was initially dissolved in water, followed by the addition of IND. Tween® 80, at 1 %

of the total mass of CIC intended for suspension, was then incorporated to stabilize the hydrophobic drug. In both the solution and suspension formulations, IND and CIC were added at concentrations of 0.833 % and 0.533 %, respectively, corresponding to 125 μg of IND and 80 μg of CIC in a 15 mg powder. These concentrations were selected based on the clinical dosages of the two compounds when administered separately on the market. To achieve this, at a 5 % (w/v) solid content with fixed proportions of excipient and API, the preparation of 100.0 mL feedstock requires 41.40 mM of Crysmeb and 35.55 mM of HPβCD. Under these conditions, the targeted amount of CIC for complexation is 26.65 mg.

2.6. Spray-drying of the liquid preparation

Powders were produced by spray-drying SOL_{Crysmeb} and SUS_{HPβCD} with concentrations of 5 and 10 % (w/v) using the Procept 4 M8-Trix Formatrix spray-dryer (Procept, Zelzate, Belgium) equipped with a bi-fluid nozzle. The resulting mixtures were atomized under the following conditions: an inlet temperature of 160°C , a feed flow rate of 3.85 g/min, a nozzle gas pressure of 3 bar, a cyclone gas pressure of 0.4 bar, an inlet gas flow of $0.4 \text{ m}^3/\text{min}$, and a nozzle diameter of 0.4 mm. These parameters were established based on previous research aimed at engineering ultra-light microparticles, facilitated by the deflated shape of cyclodextrin (Lechanteur et al., 2023). The process yield for each formulation was calculated using the equation provided in Eq. (1).

2.7. Characterization of the dried powders

2.7.1. Particle size distribution (PSD)

The particle size distributions (PSDs) of the powders were determined by laser diffraction using the Malvern Mastersizer 3000® (Malvern Instruments, Worcestershire, UK), equipped with an AeroS unit. A standard Venturi was utilized to disperse a quantity of powders equivalent to a spatula tip on the micro tray, accommodating the low material quantity. The feed rate was set at 30 %, with an air pressure of 4.0 bar, to achieve the required obscuration range of 0.5–8.0 %, resulting in a sample measurement duration of 10 s. The Malvern Mastersizer software was used to analyze the particle size of the powders. Three replicates of each sample were measured to determine the average PSD.

2.7.2. Residual moisture content

The residual water content of all powders was assessed rapidly after spray-drying using Thermogravimetric Analysis (TGA; Perkin Elmer, Norwalk, CT). Powder samples ranging from 8 to 13 mg were placed on a platinum sample pan and heated from 25 to 150°C at a rate of 10°C/min . TGA is employed to assess the mass loss of a sample when subjected to elevated temperatures that surpass the evaporation point of water. A decrease in the mass of the sample is recorded as water evaporates, enabling the quantification of the moisture content in the analyzed powders.

2.7.3. Particle morphology

Particulate morphology was analyzed using scanning electron microscopy (SEM) with either a Philips XL30 ESEM or an FEI Quanta 600, after metallizing the samples with approximately 50 nm of gold. Representative micrographs were captured, and approximately ten particles from each powder were randomly selected for detailed morphological analysis. Additionally, the average number of dimples

(Nd) was manually counted, assuming that the visible dimples represent approximately half of the total number on a particle. The dimple depth (DepthD) was then estimated by measuring the distance from the deepest point of the dimple to the highest point of the surrounding surface, normalized to the diameter (d) of the particle. This measurement was conducted using image analysis tools, with the depth of each visible dimple carefully quantified and averaged across the sampled particles (Lechanteur et al., 2022).

2.8. Evaluation of dried powders homogeneity

2.8.1. Relative standard deviation (RSD) determination

The uniformity of each produced powder was assessed by collecting 10 samples from various locations within the powder bed, covering the entire surface and depth. These powders were stored at room temperature and shielded from light. Each sample, containing approximately 20 \pm 1 mg of SD powder, was dissolved in methanol, allowing for the determination of CIC and IND concentrations using HPLC, as presented in Section 2.2. The recovery rate was evaluated using the specified equation below (Eq. (2)). Blend uniformity was determined by calculating the relative standard deviation (RSD) from the 10 samples. This metric represents the ratio of the standard deviation to the mean, expressed as a percentage. Powders with an RSD of \leq 5 % for the mean CIC and IND recovery rates were deemed homogeneous, according to the guidelines established by the European Pharmacopoeia for assessing the uniformity of powders.

$$\text{Recovery rate (\%)} = \frac{\text{Quantified drug content}}{\text{Theoretical drug content}} \cdot 100 \quad (2)$$

2.8.2. Raman microscopy

Raman hyperspectral imaging (R-HSI) was conducted using a Labram HR Evolution (Horiba Scientific) system, which included an EMCCD detector with a 1600 \times 200-pixel sensor (Andor Technology Ltd.). The setup featured a Leica 50x Fluotar LWD objective, a 300 gr/mm grating, and a 785 nm laser (45 mW output) sourced from a Toptica Photonics XTRA II single frequency diode laser. A 25 % neutral density filter was used to reduce light intensity and avoid sample damage. Spectral data, obtained by averaging two acquisitions of 2 s each, covered the range from 463 to 1853 cm^{-1} .

For consistency, raw materials were characterized under the same conditions as the mapping experiments. Prior to imaging, the powders were compressed using a Specac 5 mm pellet die with a 0.5 T load. Mapping consisted of a 75 \times 75 pixels grid with a 2 μm step size, resulting in a total area of 150 \times 150 μm^2 . Raw spectral data underwent preprocessing via PCA denoising and baseline adjustments with Asymmetric Least Square correction (parameters: $p = 1 \times 10^{-4}$, $\lambda = 1 \times 10^5$).

The number of pure signals in the mapping was estimated using singular value decomposition. Independent component analysis (ICA) with the JADE algorithm was used to separate the previously estimated number of pure signals: three for the suspension-derived powder (MAh17/LAC-50/50) and one for the solution-derived powder (HPBCD-100). These results were validated by comparing the ICA loadings to spectra from pure components. Among the three ICs separated for the suspension data, one IC represented highly noisy pixels and was discarded for subsequent analyses.

2.9. In vitro lung deposition determination

2.9.1. Next generation Impactor (NGI)

The aerosol performance *in vitro* was assessed using a Next Generation Impactor (NGI; Apparatus E, Copley, Nottingham, UK), in accordance with the European Pharmacopoeia guidelines. This impactor, consisting of eight stages, includes a pre-separator, and the induction port is connected to the device via an appropriate mouthpiece adapter.

Airflow was regulated to 60 or 100 L/min by a flow controller (TPK; Copley, Nottingham, UK) for 2.4 s at each flow rate. The study employed the Onbrez® Breezhaler® (Novartis Pharma AG), a device characterized by low resistance, with 12 capsules tested per run. The powder deposited on each stage, including the mouthpiece, capsules and device, was collected using methanol and subsequently analyzed by HPLC after sonication to complete APIs solubilization. The recovery dose (RD) denoted the total amount of API retrieved from the capsules and the device up to the final stage of the NGI. The emitted dose (ED), representing the percentage of the drug released from the inhaler, was calculated from the cumulative quantity of powder from the induction port to the final NGI stage. The fine particle dose (FPD) was defined as the mass of the drug with an aerodynamic diameter of less than 5 μm . The fine particle fraction (FPF) was calculated based on the emitted dose, as no changes were made to the inhaler used throughout the study and was determined using the following equation. (Eq. (3)).

$$\text{FPF (\%)} = \frac{\text{Mass of particles} < 5 \mu\text{m}}{\text{Emitted dose (ED)}} \cdot 100 \quad (3)$$

The Mass Median Aerodynamic Diameter (MMAD) was derived from the cumulative aerosol mass distribution curve, representing the diameter through which 50 % of the total aerosol mass can pass. The Geometric Standard Deviation (GSD) was determined using the ratio of the diameters at the 84th percentile (D84) and the 50th percentile (D50). Additionally, the pulmonary deposition results of our powders, specifically focusing on IND deposition, were compared to those of Onbrez®, a DPI formulation marketed in Belgium that utilizes lactose as a carrier and contains IND.

2.9.2. PreciseInhale®

The PreciseInhale®, as previously described in detail (Gerde et al., 2004; Malmjöf et al., 2019; Selg et al., 2013), is an innovative inhalation exposure platform which allows to investigate how inhaled particles act in the lungs. This machine enables aerosol exposures to a wide range of *in vitro*, *ex vivo* and *in vivo* models, using a small amount of raw substance to generate aerosols in a free-flowing, fine particulate stream and producing repeatable data (Fioni et al., 2018). The PreciseInhale® system offers several different aerosol sources which can be used according to the study's goal: micronized dry powders (Gerde et al., 2004), solutions (nebulizers) and clinical inhalers, such as DPIs and pMDI (Gerde et al., 2020). In the current study, the PreciseInhale® dry powder inhaler setup was used to analyze the test powders' dispersibility, aerodynamic performance and PSD, and to eventually compare these data with those generated with the NGI.

The PreciseInhale® dispensing system (Inhalation Sciences AB, Huddinge, Sweden) was used to generate powder aerosols (Supplementary data A). Powder samples were loaded into empty DPI capsules (Capsugel Zephyr, Lonza, Verviers, Belgium) in carefully weighed doses of around 1 mg. The sample-filled capsules were actuated in the dry powder inhaler of the specialty Onbrez® Breezhaler® (Novartis Pharma BV, Basel, Switzerland), with an inhalation flow of 60 L/min and a corresponding pressure drop of 4 kPa over the inhaler. The actuation time to ideally place the inhaler puff in the 300 mL holding chamber at the chosen actuation flow rate was calculated by equation B.1 (Supplementary data B).

Following actuation, the flow direction in the holding chamber was reversed and an exposure air flow of 400 mL/min was employed to draw the aerosol through the Casella and to enable the collection of the test powders' aerosols for analysis. Moreover, a pre-exposure aerosol mixing period of 0.6 s was chosen for all exposures, and exposure times of 90 s for the yield determination and 120 s for the particle size determination were applied.

The aim of the aerosol-generation procedure with the PreciseInhale® was to assess the flowability, dispersibility and aerodynamic PSD of the spray-dried formulations. The flowability and dispersibility were

measured as the Casella maximum concentration (C_{\max}) and as the amount of aerosol likely to be deposited on the inhalation filter (M_{cas}) (Selg et al., 2013; Xu et al., 2022).

The yield was calculated as the weight difference of the end filter (25 mm GF/A end-filters, Inhalation Sciences, AB, Huddinge, Sweden) before and after aerosol exposure, divided by the powder dose shot in the machine, according to the following equation (Eq. (6)):

$$\text{Aerosolyield}(\%) = \frac{\text{Endfilterafterexposure}(\text{mg}) - \text{Endfilterbeforeexposure}(\text{mg})}{\text{Powderdoseloadedinthecapsule}(\text{mg})} \cdot 100\% \quad (6)$$

To calculate the C_{\max} , the M_{cas} and the yield, five measurements were performed for each formulation.

MMAD, GSD and PPF were measured by cascade impaction analysis with the use of a 9-stage Marple Cascade Impactor (CI) (MSP Corporation, Shoreview, MN, USA), attached to the exposure outlet of the PreciseInhale®. PPF was calculated as the ratio of the weight of fine particles with a diameter below 5 μm and the total weight of the powder recovered on all the 9 filters of the Marple cascade impactor, according to the following equation (Eq. (7)):

$$\text{Fineparticlefraction}(\text{PPF}, \%) = \frac{\text{Weightofparticles} < 5\mu\text{m}(\text{mg})}{\text{Recoverydose}(\text{mg})} \cdot 100 \quad (7)$$

The aerodynamic PSD measurements were performed according to the provider's instructions. Following the inhaler actuation cycle, a reversed exposure flow rate of 2000 mL/min was employed to draw the aerosol from the holding chamber through the CI. According to their particle size, the powders impacted on the stages of the CI and were captured on the filters (Cascade Impactor, stage 1–8 filter, GF/A; Cascade Impactor, end-filter, GF/F, Inhalation Sciences, AB, Huddinge, Sweden). The MMAD, GSD and PPF were calculated by gravimetric measurement (Microbalance XP26, Mettler Toledo). The experiments were performed in triplicate for each formulation. The recovery of the PSD measurements was also calculated as the ratio of the weight of the 9 filters in the CI stages before and after exposure and the total weight of powder shot in the CI, according to the following equation (Eq. (8)):

$$\text{Recovery}(\%) = \frac{9\text{CIfiltersafterexposure}(\text{mg}) - 9\text{CIfiltersbeforeexposure}(\text{mg})}{\text{Totalpowderdoseloadedinthecapsules}(\text{mg})} \cdot 100 \quad (8)$$

The recovery refers to the collection efficiency of the aerosolized particles after they have been generated by the PreciseInhale® system, and it determines how much of the aerosolized material is captured on the Marple Cascade Impactor stages.

A LabVIEW based proprietary software (National Instruments, Austin, TX) of Inhalation Sciences AB is used by the PreciseInhale® platform to manage both execution of aerosol exposure cycle and exposure data acquisition of pressure, airflow, and aerosol concentration (Ewing et al., 2021).

Fig. 1A and 1B provide a schematic representation of the functioning of the PreciseInhale® system in the dry powder inhaler configuration. The PreciseInhale® system in the dry powder inhaler setup is represented in Supplementary data C.

2.10. Stability studies

Stability studies of the optimized 10 % (w/v) powder were conducted at controlled room temperature ($25^\circ\text{C} \pm 2$, $60\% \pm 5\text{ RH}$) and under accelerated conditions ($40^\circ\text{C} \pm 2$, $75\% \pm 5\text{ RH}$) following ICH (International Council for Harmonisation of Technical Requirements for Pharmaceuticals for Human Use) guidelines. The powder was stored in

sealed vials and subjected to the specified climate conditions. Samples were taken at 1, 2, 3 and 6 months after being placed in the stability chamber. The powders were inspected for signs of caking or discoloration, and analyses of drug content, moisture content, and particle size were performed periodically. Impaction studies utilizing the NGI were performed after a 6-month period.

2.11. Statistical analysis

All data were statistically analyzed using GraphPad Prism software (version 8.4.3, La Jolla, CA, USA) and are expressed as mean \pm standard deviation (SD). Statistical significance was determined using ANOVA, followed by Tukey's multiple comparisons test. A p-value of ≤ 0.05 was considered statistically significant.

3. Results and discussion

3.1. Characterization of the cyclodextrin-ciclesonide complexes

Considering the low aqueous solubility of ciclesonide, a highly hydrophobic ICS with a solubility in water less than 0.5 mg/L at room temperature (Takeda Canada Inc., 2012), various cyclodextrins were tested to compare the atomization of a feedstock, where the CIC was solubilized on one hand and suspended in the liquid on the other.

According to the phase-solubility diagram classifications by Higuchi and Connors, the solubility diagrams for CIC complexation with all tested cyclodextrins, shown in Fig. 2, correspond to A-type profiles

(Saokham et al., 2018). These diagrams demonstrate a proportional increase in CIC solubility with rising cyclodextrin concentration. Within the 0 to 200 mM cyclodextrin range, the apparent water solubility of CIC increases linearly, attributed to the formation of a soluble 1:1 inclusion complex with the tested carbohydrates. Among them, the methylated cyclodextrin Crystmex shows superior encapsulation efficiency for CIC compared to HP β CD and HP γ CD.

The results indicate that, at the cyclodextrin concentrations required to prepare a 5 % (w/v) feedstock (35.55 mM Crystmex, 31.29 mM HP γ CD, and 31.29 mM HP β CD), Crystmex exhibits the capacity to complex up to 10 times more CIC than HP β CD. This can be explained by the fact that CIC complexation with cyclodextrins is closely related to the hydrophobicity of their cavities. Indeed, Crystmex exhibits the highest hydrophobic cavity, as methyl substitutions increase the apolar character of the cavity by repelling water molecules. In contrast, HP β CD,

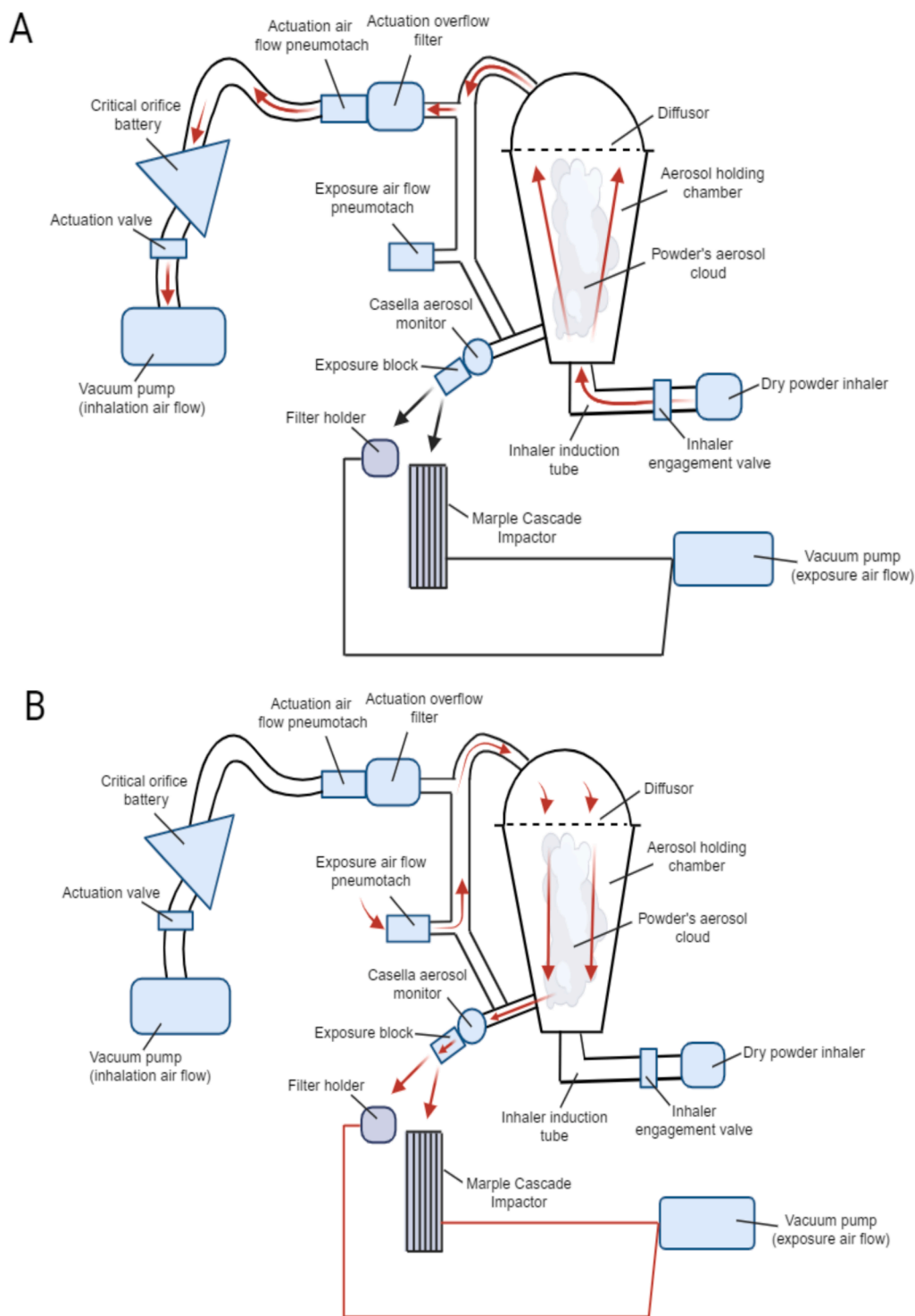


Fig. 1. A schematic overview of how the PreciseInhale® system works in the dry powder inhaler setup. Red arrows show the direction of the inhalation flow (A) or exposure flow (B). 1 mg of powder is loaded in DPI capsules and actuated in the dry powder inhaler coupled to the PreciseInhale®'s inhaler induction tube. The inhalation air flow is provided by the critical orifice battery and its vacuum pump (A). The aerosol settles in the holding chamber, and it is drawn towards the exposure target by the air flow supplied by the exposure air flow vacuum pump (B). The Casella Microdust Pro measures the aerosol concentration during the procedure. The exposure modules used in the current project were the filter holder for the yield, Cmax, Mcas determination and the Marple cascade impactor for the particle size distribution analysis (MMAD, GSD, FPF). The PreciseInhale® also has four fast acting pneumatic pinch valves which control pressure build-up and release as well as the correct direction of the airflow. These valves have been omitted for clarity in the overview. A detailed description of the PreciseInhale® system can be found in reference (Gerde et al., 2004).

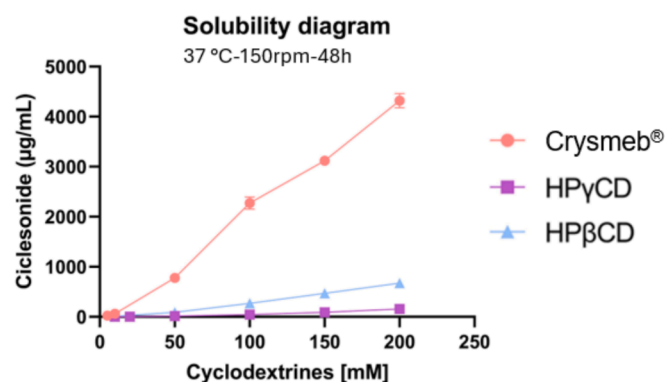


Fig. 2. Phase solubility diagram of Ciclesonide in complexation with Crystmeb®, HPβCD, HPγCD. Analysis was performed in triplicates ($n = 3$) and values are presented as mean and standard deviation.

Table 1
Summary of the composition of the atomized formulations.

	DPI-SOL _{Crystmeb}	DPI-SUS _{HPβCD}
Feedstock nature	Solution	Suspension
Excipient nature	Crystmeb	HPβCD
Other component	/	Tween 80
Excipient (%)	98.634	
CIC (%)	0.533	
IND (%)	0.833	

due to its hydroxypropyl substitutions, presents a more hydrophilic cavity that enhances overall aqueous solubility but reduces the ability to effectively complex highly lipophilic drugs, as these groups partially interact with water at the cavity entrance (Santos et al., 2017). Finally, HPγCD, with its larger cavity, permits greater water access, making it the least hydrophobic. These structural differences likely account for the superior complexation capacity of Crystmeb towards CIC (Aiassa et al., 2023).

Based on these findings, Crystmeb will be used to complex CIC to produce a solution that will subsequently be atomized to generate powders designated as DPI-SOL_{Crystmeb}. Similarly, HPβCD will be employed to create a suspension and upon drying, this powder is named DPI-SUS_{HPβCD}. A recap of the dried formulations investigated in this

study is provided in the following table (Table 1):

In addition to studying the comparison of the influence of the APIs solubilization state on the properties of the developed powders, the effect of increasing the solid content from 5 to 10 % (w/v) will be investigated. The atomization of Crystmeb under optimal drying parameters will also be evaluated to determine whether this cyclodextrin enables the development of a DPI that improves lung deposition, similar to the results obtained with HPβCD in previous studies by Dufour et al. (Dufour et al., 2015) and Lechanteur et al. (Lechanteur et al., 2023).

3.2. Impact of feedstock nature on powder properties

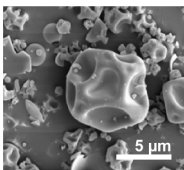
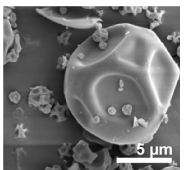
The physicochemical properties of the powders obtained from dried solutions (DPI-SOL_{Crystmeb}) and suspensions (DPI-SUS_{HPβCD}), with solid particle concentrations of 5 and 10 % (w/v), are presented in Table 2.

Firstly, regarding the SD process yield, values remained relatively high across most tested conditions, averaging around 77 %, emphasizing minimal powder losses during the drying process.

The powders' water content ranged between 4.34 and 6.46 % (Fig. 3B) which theoretically supports API stability and optimal lung deposition (Behboudi-Jobbehdar et al., 2013). These residual moisture levels help mitigate issues related to excessive electrostatic charge and particle aggregation, issues already present due to the powder's hygroscopic properties (Lechanteur and Evrard, 2020). The results show that an increase in the solid concentration of the matrix decreases the residual moisture content in the resulting particles by raising the ratio of solute to water within each drying droplet, promoting more efficient water removal during drying (LeClair et al., 2016). This effect led to a significant ($p < 0.05$) decrease in water content, dropping from 6.46 to 4.74 % as solid content increased. Interestingly, at a lower solid concentration of 5 % (w/v), suspension-derived powders showed ($p < 0.05$) lower water content of 4.34 % compared to the 6.46 % from the solution-derived ones. This may be attributed to the presence of suspended drug particles in the liquid feed prior to atomization, which are consequently present within the generated droplets during drying. These solid particles can reduce water retention during drying, resulting in lower moisture content in the final powders. Yet, at a 10 % solid content, no significant differences were observed between dried solutions and suspensions.

As previously highlighted, assessing particle size is crucial for developing inhalable powders. To ensure deep lung deposition, particle sizes should lie from 1 to 5 μm. According to Ou et al. (Ou et al., 2020),

Table 2
Properties of developed powders from atomized solutions (DPI-SOL_{Crystmeb}) and suspensions (DPI-SUS_{HPβCD}), at solid content of 5 and 10 % (w/v). Analyses were performed in triplicates ($n = 3$) and results are presented as mean ± standard deviation.

	DPI-SOL _{Crystmeb}		DPI-SUS _{HPβCD}	
Feedstock nature	Solution		Suspension	
Solid content (%) (w/v)	5	10	5	10
Process yield (%)	77.60 ± 1.03	77.29 ± 1.26	77.39 ± 2.82	65.85 ± 10.39
Particle size (μm)				
d_{10}	1.27 ± 0.08	1.30 ± 0.04	1.38 ± 0.04	1.59 ± 0.11
d_{50}	2.94 ± 0.04	2.99 ± 0.12	3.45 ± 0.21	4.12 ± 0.22
d_{90}	6.33 ± 0.11	5.89 ± 1.49	7.73 ± 0.48	10.01 ± 1.36
Span	1.72 ± 0.02	1.70 ± 0.07	1.84 ± 0.05	2.05 ± 0.36
Water content (%)	6.46 ± 0.54	4.74 ± 1.01	4.34 ± 0.21	4.62 ± 0.67
Morphology (FoV 20)				
Number dimples (Nd) (–)	10.57 ± 1.90	11.75 ± 2.91	11.75 ± 2.49	11.5 ± 4.99
Depth dimples/d (Dd) (–)	0.28 ± 0.07	0.19 ± 0.03	0.25 ± 0.07	0.23 ± 0.08

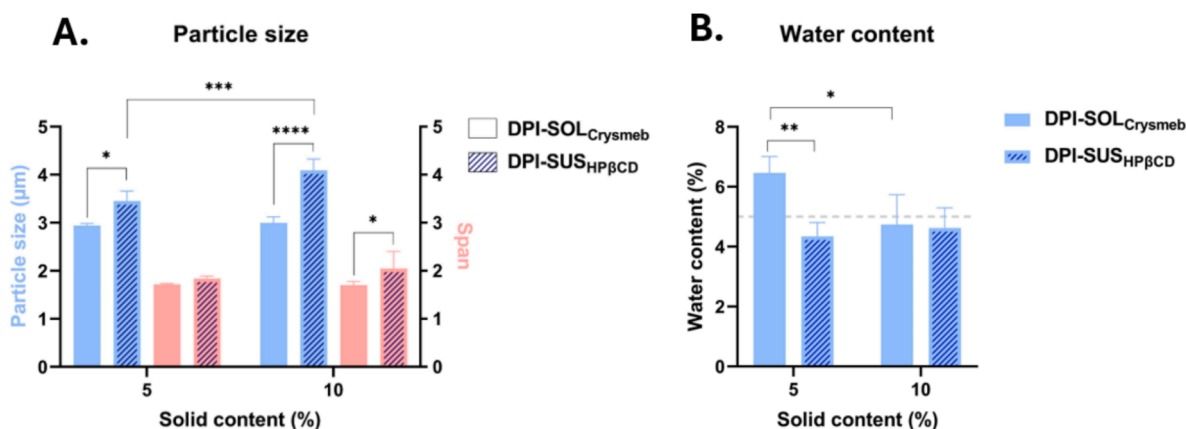


Fig. 3. Particle size (A) and water content (B) of all produced powders from atomized solutions and suspensions, at both solid content of 5 and 10 % (w/v). Analyses were performed in triplicates ($n = 3$) and values are presented as mean \pm standard deviation.

particles with a size of approximately 3 μm are considered optimal for enhanced deposition. The powders produced in this study, especially for DPI-SOL_{Crysmeb}, met these criteria, displaying particle sizes close to 3 μm (Fig. 3A). Conversely, DPI-SUS_{HPβCD}, particularly at 10 % solid content, exhibited considerable ($p < 0.05$) larger particles (4.12 μm) compared to solutions (2.99 μm). Due to the presence of hydrophobic drug solid particles within the droplets during suspension atomization, in contrast to solutions where all components are dissolved, the likelihood of obtaining larger particles upon drying is increased. Moreover, for atomized suspensions, higher solid content further amplified particle sizes, ranging from 3.45 μm at 5 % to 4.12 μm at 10 %. This is likely due to the increase in solid concentration per droplet under identical drying conditions (W.D. Wu et al., 2014).

Finally, regarding particle morphology, deflated structures were observed in all powders, appearing to be suitable for improved DPIs aerosolization efficiency and lung deposition (Chew and Chan, 2001; Vehring, 2008). Focusing on the influence of increased solid content on particle morphology, literature indicates that higher solid generally tends to promote more spherical particles by accelerating crust formation, providing greater resistance to deformation (W.D. Wu et al., 2014). Additionally, studies highlighted that at higher feed concentrations, formation of SD particles with greater porosity and lower bulk density are obtained, due to reduced solvent in each droplet and faster evaporation times (Littringer et al., 2012). In this study, no morphological changes were observed whatever the solid content. However, in comparison to typical DPI production atomized with around 1 % solid content, the high feed concentrations will result in faster production

times which represents a considerable interest from an industrial standpoint.

Furthermore, previous investigations have highlighted the Péclet number (Pe) as a determinant of particle morphology (Dufour et al., 2015; Vehring et al., 2007). High molecular weight excipients, such as HPβCD (1541.5 g/mol), are associated with higher Pe values and have been shown to promote the formation of deflated particles at optimized drying parameters, in contrast to lower molecular weight excipients like mannitol (182.2 g/mol) (Lechanteur et al., 2022). Interestingly, in this study, the nature of the cyclodextrin, whether originating from dried solutions or suspensions, did not significantly influence particle morphology or the measured morphological parameters (Nd and Dd). Crysmeb cyclodextrin was dried for the first time under optimized conditions, and the results confirmed that its high molecular weight (1191 g/mol) likely contributed to a high Pe value, leading to the successful formation of deflated, ball-shaped particles (Truffin et al., 2024).

3.3. Impact of feedstock composition on powders homogeneity and drug recovery

Following the drying process and the evaluation of powders properties, the recovery rate of both active substances from the resulting powder was assessed to evaluate any potential degradation of the drug, due to the drying process temperature, or the influence of its solubilization state. Fig. 4A shows that most powders unveil recovery rates between 95 and 105 %, indicating no significant APIs losses during the drying process (Das et al., 2009), independently of the solid content.

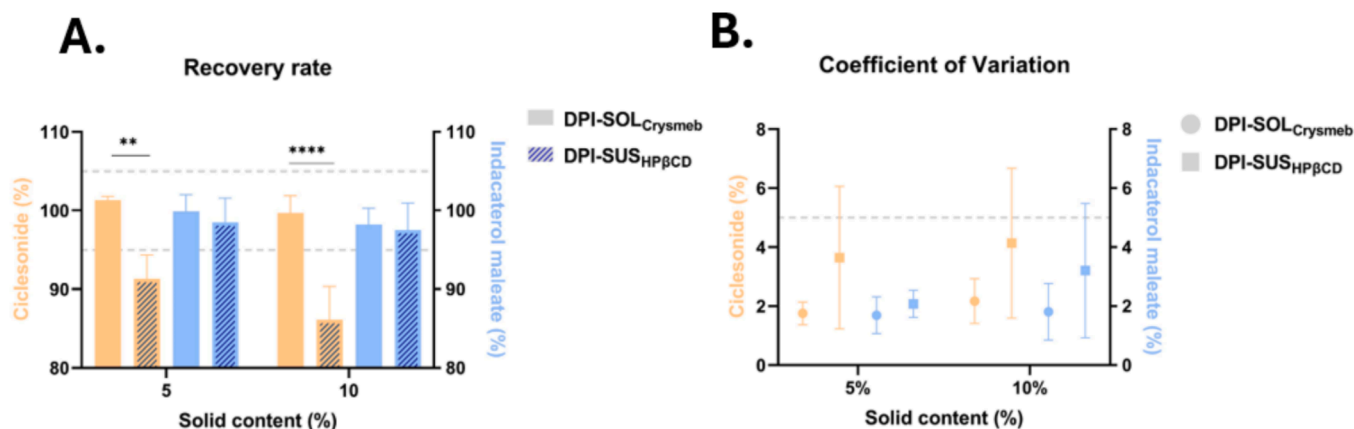


Fig. 4. A) APIs recovery rate post-drying from atomized solutions (DPI-SOL_{Crysmeb}) and suspensions (DPI-SUS_{HPβCD}), at both tested solid content (5 and 10 % (w/v)). B) Coefficients of variation for APIs across 10 samples from atomized solutions and suspensions, at both tested solid contents (5 and 10 % (w/v)). Analyses were performed in triplicates ($n = 3$) and values are presented as mean \pm standard deviation.

However, CIC recovery rates in atomized suspensions were significantly lower reaching only 91.30 % (± 3.05) and 86.11 % (± 4.26) ($p < 0.05$), at 5 and 10 % solid content respectively. This observation is hypothesized to be due to its non-solubilized state, which may lead to particle adhesion to the spray dryer and consequently reduced recovery rates. The decrease in the recovery rate of the hydrophobic molecule in atomized suspensions is proposed to be attributed to the solubilization state of the feed liquid rather than thermal degradation since the degradation temperature for CIC was 354 °C and the atomization process temperature of 160 °C. The thermal degradation of IND (203 °C) and its soluble state make it unsurprising that no degradation is observed upon drying (thermal degradation TGA curves of CIC and IND are shown in [Supplementary data D](#)).

Moreover, in DPIs development, API typically constitutes a small fraction of the total powder mass. To ensure consistent therapeutic efficacy and minimize adverse effects, each dose of the inhaled product must deliver an identical number of active substances ([Marianni et al., 2021](#)). The uniformity of powder homogeneity was evaluated using the RSD calculated based on the API content after drying. Dose uniformity in DPIs is considered acceptable when the RSD is less than 5 % ([Nguyen et al., 2015](#)).

[Fig. 4B](#) shows CiCs distribution within 10 samples and indicates a RSD of 1.76 % (± 0.38) and 2.17 % (± 1.94) for atomized solutions (DPI-SOL_{Crysmeb}) with solid contents of 5 and 10 %, respectively, and 3.65 % (± 2.42) and 4.13 % (± 4.24) for atomized suspensions (DPI-SUS_{HPβCD}) at the same solid contents. Similarly, INDs distribution exhibited an RSD of 1.69 % (± 0.62) and 2.08 % (± 0.46) for atomized solutions at 5 and 10 % solid content, and 2.08 % (± 0.45) (5 % solid content) and 3.21 % (± 3.47) (10 % solid content) for atomized suspensions. Homogeneity appears to be maintained when atomizing solutions, regardless of the solid content. However, when non-solubilized particles are atomized, the RSD tends to increase particularly for hydrophobic particles, which could be attributed to reduced product homogeneity resulting from the random distribution of suspended particles into aerosolized droplets during atomization ([Chow et al., 2020](#); [Khanal et al., 2022](#)).

Further analysis was performed using Raman hyperspectral imaging (R-HSI) to investigate the distribution of the components within the SD powders. For dried solutions, the imaging revealed a single Raman signature for each pixel across the sample, as shown in [Fig. 5A](#). This spectral uniformity indicates a homogeneous and intimate distribution of the excipient and API, attributed to their complete solubilization prior to the atomization process. In contrast, the analysis of atomized suspensions showed distinct signatures corresponding to the CIC non solubilized particles ([Fig. 5B](#)). These particles, with a D0.5 of 1.81 μm,

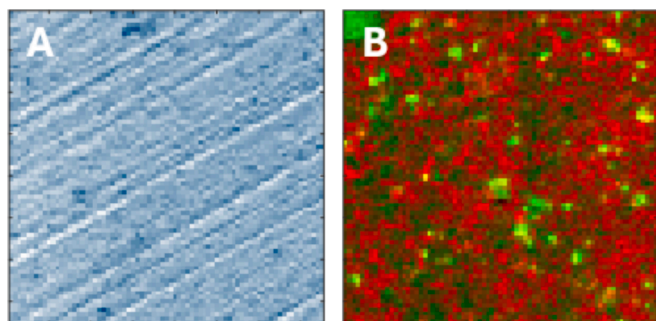


Fig. 5. Raman hyperspectral imaging results (following ICA analysis) were obtained for powders produced from an atomized solution (DPI-SOL_{Crysmeb}) (A) and an atomized suspension (DPI-SUS_{HPβCD}) (B), respectively. In the imaging for the solution (A), the blue color represents a single signature observed uniformly across all pixels, indicative of homogeneity. The texture of the image is resulting from sample surface imperfections. In contrast, in the imaging for the suspension (B), red and green colors correspond to distinct signatures attributed to the excipient HPβCD and the hydrophobic CIC, respectively, reflecting a less uniform distribution.

closely match the green dots observed in the imaging data, which are approximately the size of a single pixel (2 μm × 2 μm). These results highlight a less uniform distribution of CIC particles within the final product, likely caused by incomplete solubilization and the uneven distribution of suspended particles into droplets during atomization of the hydrophobic substance before atomization and subsequent drying ([Chow et al., 2020](#); [Khanal et al., 2022](#)).

This difference in API repartition underscores the influence of the initial solubilization state on the final distribution of components within the powder, resulting in distinct impacts on the uniformity of the excipient and API distribution ([Paudel et al., 2013](#)).

3.4. *In vitro* aerosolization performance

In this study, the *in vitro* aerodynamic performance of produced powders was evaluated using two distinct impaction methods. First, the cascade impaction method with NGI equipment which is a conventional assay described in the European Pharmacopeia, and second, the PreciseInhaler® system, an innovative and less widely known technique focusing on aerosolization performance.

3.4.1. Impact of solid content and drugs solubilization state on DPIs *in vitro* aerodynamic performance

To further investigate the impact of solid concentration and drugs solubilization state on DPI performances, the lung deposition potential of all produced powders was evaluated using the NGI. All data overviews from the impaction studies on atomized suspensions and solutions, at solid concentrations of 5 and 10 % (w/v), are presented in [Table 3](#). The aerodynamic particle size distribution profile of CIC and IND from DPI-SOL_{Crysmeb} and DPI-SUS_{HPβCD}, at both solid content of 5 and 10 % (w/v) are represented in [Supplementary data E A-B](#).

According to the results, atomized solutions produced significantly ($p < 0.05$) higher lung deposition for both APIs compared to atomized suspensions, as indicated by the FPF values. For CIC, the FPF reached 64.43 (± 8.46) and 68.05 % (± 8.64) for atomized solutions at 5 and 10 % (w/v), respectively, compared to 37.12 (± 4.10) and 29.66 % (± 5.42) for atomized suspensions. Similarly, IND showed increased lung deposition with atomized solutions, achieving an FPF of 59.68 (± 4.33) and 60.39 % (± 4.42) for powders at 5 and 10 % (w/v), respectively, compared to 46.99 (± 6.06) and 41.05 % (± 7.39) for atomized suspensions.

This difference is primarily attributed to the higher Mass Median Aerodynamic Diameter (MMAD), which considers particle morphology and density, whereas D0.5 is a value that describes the particle size and is based on the assumption of spherical particle geometry.. Both MMAD and D0.5 indicate that atomized suspensions result in larger particles, as reflected by higher values. Larger particles, as shown in [Fig. 6A-B](#), increase impaction in the upper respiratory tract, reducing deposition in deeper lung regions and resulting in lower FPF. Conversely, the Geometric Standard Deviation (GSD), which measures aerodynamic particle size dispersion, remained low for all powders, indicating uniformity in aerodynamic diameter (Dae).

Regarding the Emitted Dose (ED), all powders achieved values exceeding 90 %. However, powders produced from atomized suspensions tended to exhibit higher ejection efficiency from the capsule during inhalation. While the nature of the excipients could have been a contributing factor, both cyclodextrins used in this study share similar morphological properties. This phenomenon can then be due to the larger particle size of powders from atomized suspensions, improving powder flowability, thereby leading to increased ED. Nonetheless, this larger size also led to greater API loss in the throat, increasing the risk of undesirable effects.

Furthermore, despite varying API doses, all developed powders demonstrated homogeneous deposition of both APIs across pulmonary stages. However, powders from atomized solutions exhibited more uniform lung deposition with similar FPF values for both APIs across

Table 3

Mean values and standard deviations of Fine Particle Fraction (FPF), Fine Particle Dose (FPD), Emitted Dose (ED), Mass Median Aerodynamic Diameter (MMAD), and Geometric Standard Deviation (GSD) for all powders produced from atomized solutions (SOL) and suspensions (SUS) with solid contents of 5 and 10 % (w/v). Analyses were performed in triplicates (n = 3) and results are presented as mean \pm standard deviation.

DPI		FPF (%)		FPD (μ g)		ED (%)		MMAD (μ m)		GSD (–)	
		SOL _{Crysmeb}	SUS _{HPBCD}	SOL _{Crysmeb}	SUS _{HPBCD}	SOL _{Crysmeb}	SUS _{HPBCD}	SOL _{Crysmeb}	SUS _{HPBCD}	SOL _{Crysmeb}	SUS _{HPBCD}
5 %	CIC	64.43	37.12	34.07	19.81	90.46	94.59	4.13	5.97	1.91	1.64
		± 8.46	± 4.10	± 1.79	± 3.45	± 0.82	± 2.25	± 0.49	± 0.21	± 0.07	± 0.03
	IND	59.68 \pm 4.33	46.99	60.05	48.35	91.00	90.83	4.24	5.21	1.92	1.66
			± 6.06	± 9.00	± 7.25	± 2.08	± 5.29	± 0.33	± 0.30	± 0.06	± 0.22
10 %	CIC	68.05	29.66	34.20	15.62	90.62	96.38	3.93	5.79	1.91	1.66
		± 8.64	± 5.42	± 2.91	± 3.45	± 2.55	± 0.85	± 0.43	± 0.96	± 0.05	± 0.10
	IND	60.39	41.05	63.22	39.80	90.45	94.74	4.05	5.11	1.90	1.68
		± 4.42	± 7.39	± 4.61	± 7.54	± 1.18	± 0.42	± 0.43	± 0.82	± 0.05	± 0.25

NGI stages, whereas atomized suspensions showed greater variability and more divergent FPF values. This uniformity is linked to the enhanced and even API distribution in powders from dried solutions, as confirmed by R-HSI analysis (Section 3.3). These results highlight the potential of atomized solutions to improve pulmonary drug delivery, ensuring consistent API availability and maximizing therapeutic efficacy.

Finally, based on the data presented in Table 3, increasing solid content from 5 to 10 % (w/v) had no significant effect on deposition values for either API, regardless of the initial atomized liquid state. Given the minimal impact of solid concentration variation on powder properties, drug recovery, and homogeneity, discussed in previous sections, the 10 % solid content was chosen for subsequent studies due to its higher drug content.

3.4.2. Impact of the flowrate on DPIs *in vitro* aerodynamic performance

When using a low resistance device, studies typically use an optimal flow rate of 100 L/min to evaluate the *in vitro* aerodynamic performance of their DPIs using the NGI. Indeed, as mentioned in the European Pharmacopoeia guidelines, the flow rate must be adapted to generate a 4 kPa pressure drop across the device, representing the mean pressure drop generated by an adult while breathing quickly and forcefully. For the Breezhaler® used in this study, Abdelalah et al. (Abdelalah et al., 2018) confirmed that a flow rate of \sim 100 L/min was needed, consistent with its low resistance design (Haidl et al., 2016). However, evaluating lung deposition at reduced flow rates is crucial to ensure that the FPF remains therapeutically sufficient. This is particularly relevant since patients with asthma and COPD show wide variability in inspiratory capacities due to disease severity and lung function differences (Wijnhoven et al., 2001). Such variability can hinder the effective use of DPIs, especially in severe cases, where achieving the required flow for optimal drug delivery is challenging, potentially compromising treatment efficacy.

Most DPIs require a minimum flow rate ranging from 30 L/min to more than 60 L/min to function optimally (Baloira et al., 2021; Hua et al., 2021). Yet, studies show that the usual flow rate for individuals using Onbrez® Breezhaler®, a DPI containing IND maleate, is around 60 L/min (Abdelalah et al., 2018).

Therefore, impaction tests were conducted on both produced powders, DPI-SOL_{Crysmeb} and DPI-SUS_{HPBCD}, at 10 % solid content, comparing results at 60 and 100 L/min. Based on the aerodynamic particle size distribution of CIC (Fig. 6A) and IND (Fig. 6B) at flow rates of 60 and 100 L/min, observations indicate increased API retention within the device at lower flow rates for both atomized solutions and suspensions. At 60 mL/min, for atomized solutions, ED values of 77.88 (\pm 2.54) and 78.23 (\pm 1.38) were observed for CIC and IND, respectively, while for dried suspensions, the values were 90.77 (\pm 0.34) and 89.30 (\pm 0.46), showing significantly ($p < 0.05$) lower emission doses compared to values at 100 L/min (Table 3). Reduced turbulence within the inhaler at lower inhalation flow rates lead to less efficient powder deagglomeration (Azouz et al., 2015; Weers, 2022). Consequently, this

results in a higher retention of the powder in the device and a lower ED, as represented in Fig. 6C.

Conversely, throat impaction was found to be reduced at lower inhalation flow rates, as slower air velocities result in less inertial deposition in the upper airways. Cuinyn et al. (Ou et al., 2020) have shown that lower flow rates decrease throat impaction, allowing the API to reach deeper regions of the lungs. In contrast, higher flow rates increase impaction in the upper respiratory tract. This is particularly relevant since many patients may have limited breathing capacities. An optimal balance must be found between maximizing API emission and minimizing throat impaction to ensure effective pulmonary drug delivery and minimized undesirable side effects.

Furthermore, no major differences in drug deposition were observed across all stages of the NGI, from the preseparator to the final stages, with variations in flow rate, particularly for atomized solutions. No significant difference was found in the FPF values for both CIC and IND in atomized solutions when the flow rate was reduced to 60 L/min, indicating that the DPI design is effectively optimized to maintain performance across varying flow rates. At the optimal flowrate of 100 L/min, the FPF values were 68.05 % (\pm 8.64) for CIC and 60.39 % (\pm 4.42) for IND, compared to 74.79 (\pm 6.40) and 71.51 % (\pm 6.62) at 60 L/min, as illustrated in Fig. 6D.

The final stage of this NGI aerodynamic performance study compared our laboratory-produced powder (10 % solid content), DPI-SOL_{Crysmeb} and DPI-SUS_{HPBCD}, with Onbrez®, a commercial DPI in the Belgian market containing indacaterol maleate and lactose. As previously noted, studies indicate that the typical flow rate for individuals using this marketed specialty is approximately 60 L/min, leading to IND FPF close to 40 % (Abdelalah et al., 2018; Horváth et al., 2017).

As shown in Fig. 6D, our atomized solution powder achieved a 10 % higher FPF than the marketed formulation, particularly at 100 L/min. These differences were not due to the inhaler device, as all formulations used the same Breezhaler®. This improved performance stems from the absence of lactose in the carrier-free formulation. In the marketed product, large lactose particles cause higher pre-separator impaction, leading to IND losses due to adhesion. Strong API-carrier interactions in the marketed formulation further reduce detachment during impaction (Abiona et al., 2022).

These results highlight the superior aerodynamic performance of powders from atomized solutions compared to current market formulations, highlighting the potential of optimized carrier-free powders for improved asthma and COPD treatment.

The findings also underscore the importance of API solubilization in achieving consistent aerodynamic performance. Powders from atomized solutions show reduced variability in API deposition across flow rates, suggesting that patients with lower inspiratory capacities (e.g., 60 L/min with the Breezhaler®) can achieve comparable therapeutic efficacy to those with higher capacities when using optimized dried solutions.

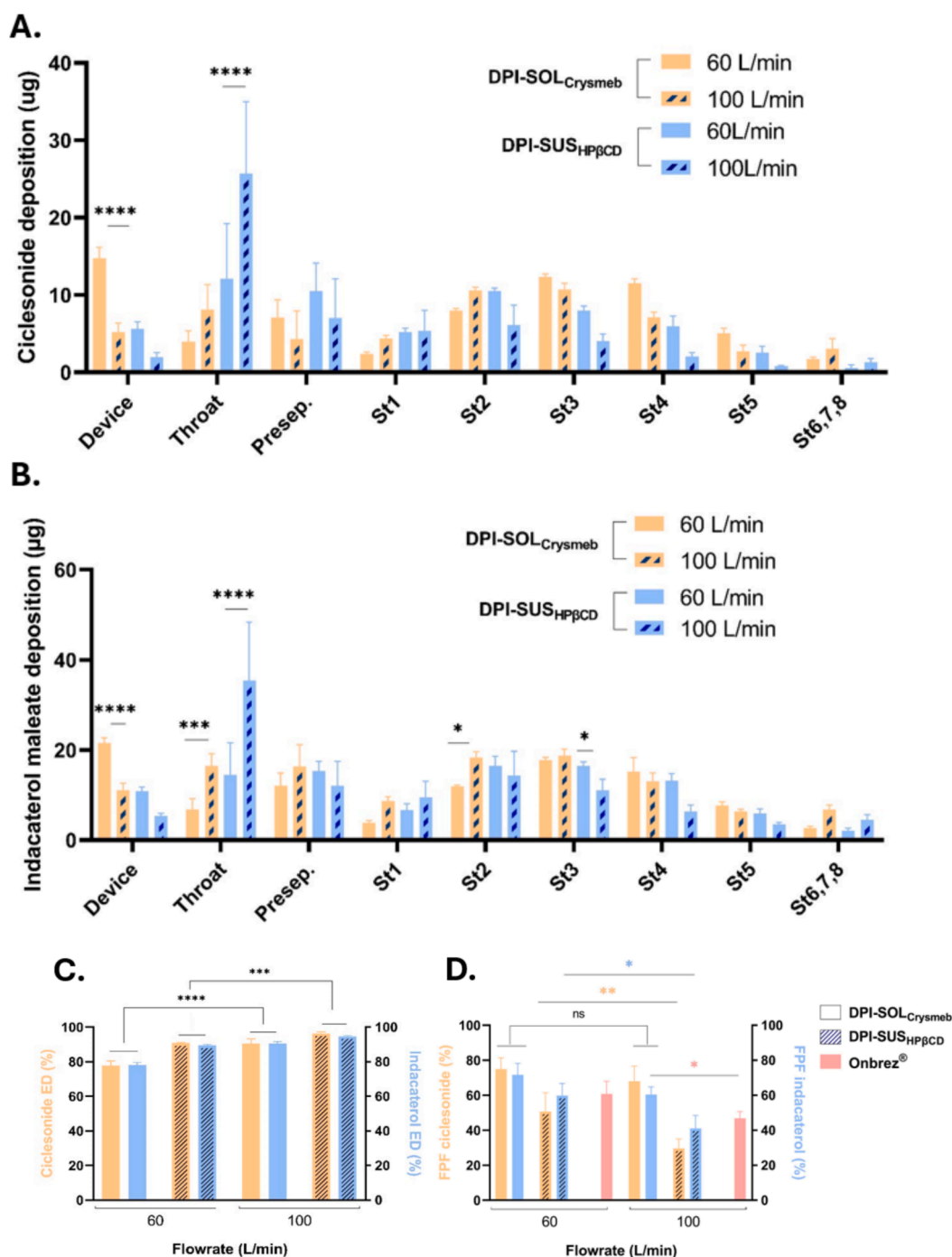


Fig. 6. A) Aerodynamic particle size distribution profile of ciclesonide (CIC) from atomized solution and suspension, at tested flow rates of 60 and 100 L/min. B) Aerodynamic particle size distribution profile of indacaterol maleate (IND) from atomized solution and suspension, at tested flow rates of 60 and 100 L/min. C) Emitted Dose comparison for both API at 60 and 100 L/min. D) Fine Particle Fraction (FPF) analysis for both API at 60 and 100 L/min. Analyses were performed in triplicates ($n = 3$) and results are presented as mean \pm standard deviation.

3.4.3. Additional characterization of powder aerodynamic properties with the PreciseInhale® system compared to NGI

In parallel to NGI, the PreciseInhale® dispensing system (Inhalation Sciences AB, Huddinge, Sweden) was used to generate the powders' aerosols. (Gerde et al., 2004; Malmjöf et al., 2019; Selg et al., 2013).

The aerodynamic performance and dispersibility of the spray-dried formulations (DPI-SOL_{Crysmeb} and DPI-SUS_{HPβCD}) were additionally evaluated with the PreciseInhale® system by measuring the C_{max} and the M_{cas} . The C_{max} refers to the maximum concentration of aerosol particles ($\mu\text{g/L}$) measured by the Casella device in the aerosol chamber

during powder dispersion. Specifically, it represents the highest recorded concentration of particulate matter during an exposure cycle and it evaluate the dispersibility of the test powder, being its ability to be effectively aerosolized and dispersed into the air (Selg et al., 2013; Xu et al., 2022). A higher C_{max} typically reflects better dispersibility of the powder under the given test conditions. The M_{cas} (μg) provides a measure of the total amount of powder that was successfully aerosolized and collected on the downstream filter during the exposure period. It offers an overall indication of the powder's aerosolization efficiency and flowability under airflow conditions, reflecting its performance in a

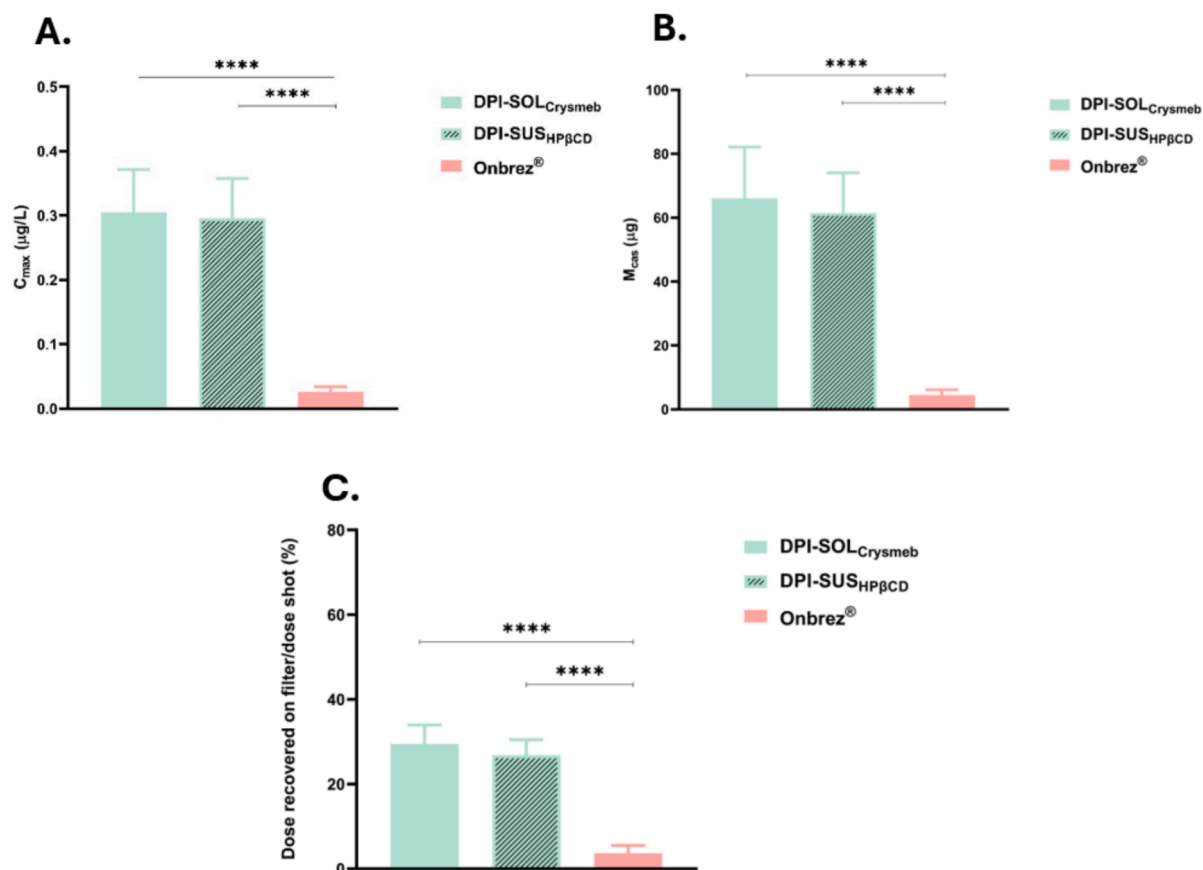


Fig. 7. (A) Aerosol performance of powder formulations from spray-dried powder from atomized solution and suspension at 10 % and the Onbrez® reference with the PreciseInhale® system. (B) Maximum concentration in Casella (C_{max}), (B) cumulative dose (M_{cas}) and (C) aerosol yield in the PreciseInhale® system for spray-dried powder formulations of indacaterol and ciclesonide tested at PreciseInhale® settings of 60 L/min/400 mL/min/4 KPa/168 ms (inhalation flow/ exposure airflow/ pressure drop/ actuation time). Data points represent three independent experiments with exposures $n = 5$, and they display mean values \pm SD. **** $p < 0.0001$ via one-way ANOVA with Tukey's post-test.

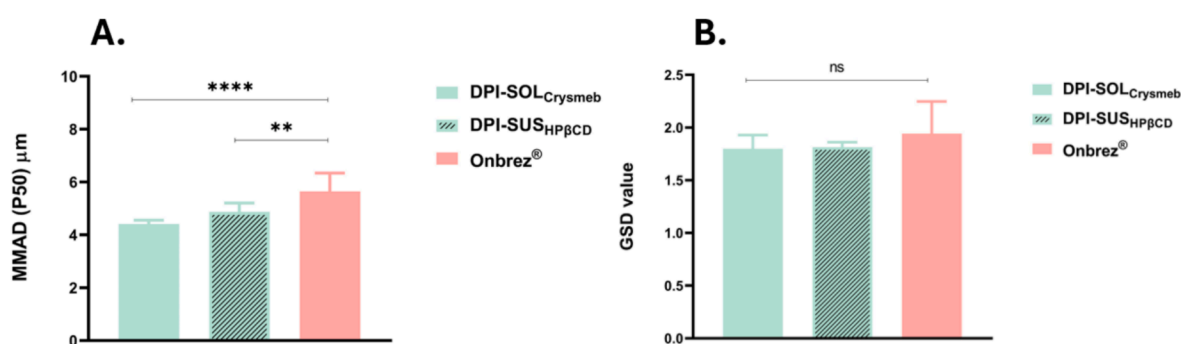


Fig. 8. (A) The mass median aerodynamic diameter (MMAD) and (B) geometric standard deviation (GSD) from spray-dried powder from atomized solution and suspension at 10 % and the Onbrez® reference with the PreciseInhale® system, based on measurements performed using a 9-stage Marple cascade impactor. Data points represent three independent experiments with exposures $n = 3$, and they display mean values \pm SD. ** $p < 0.01$, **** $p < 0.0001$ and ns: not significant via one-way ANOVA with Tukey's post-test.

dynamic, application and relevant context. By comparing M_{cas} values across different formulations, it becomes possible to assess which ones are more effectively dispersed into aerosol form and therefore exhibit superior flowability (Selg et al., 2013; Xu et al., 2022). Finally, the aerosol yield relates to the aerosol generation efficiency of the PreciseInhale® system, quantifying the proportion of the initial powder sample that is effectively aerosolized. This parameter is particularly valuable, as a low *in vitro* yield may indicate poor aerosolization performance, which could potentially result in suboptimal lung deposition *in vivo*. Furthermore, the yield (%) was calculated after each run. The

aerosol deposition properties were assessed by analyzing the particle size distribution (MMAD and GSD) of the engineered powders and by calculating the FPF (%). The commercial specialty Onbrez® Breezhaler® was used as a comparative reference.

Drawing on NGI results which investigated the influence of flow rates on powder deposition, as well as literature evidence indicating that patients using Onbrez® typically achieve an inhalation flow rate of 60 L/min (Abadelah et al., 2018), this same flow rate was selected for the PreciseInhale® experiments. At predefined settings, the powder formulations spray-dried from atomized solutions (DPI-SOL_{Crysmeb}) and

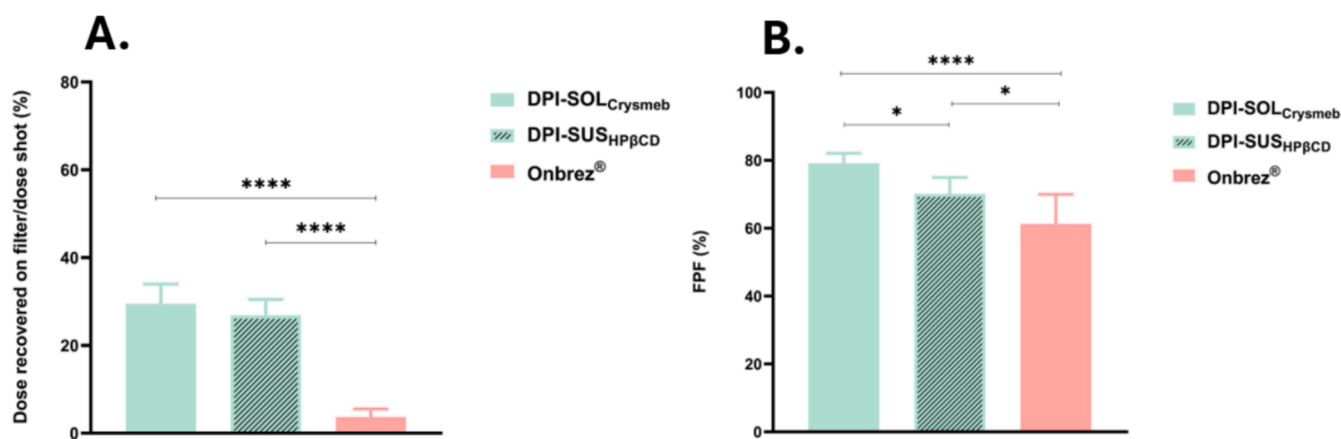


Fig. 9. (A) The recovery and (B) fine particle fraction (FPF) from spray-dried powder from atomized solution and suspension at 10 % and the Onbrez® reference with the PreciseInhale® system, based on measurements performed using a 9-stage Marple cascade impactor. Data points represent three independent experiments with exposures $n = 3$, and they display mean values \pm SD. * $p < 0.05$, and **** $p < 0.0001$ via one-way ANOVA with Tukey's post-test.

suspensions (DPI-SUS_{HPβCD}) displayed significantly higher ($p < 0.0001$) C_{max} , M_{cas} and aerosol yield compared to the reference powder Onbrez®, as represented in the Fig. 7A. This superior performance of the DPI-SOL_{Crysmeb} and DPI-SUS_{HPβCD} formulations can be attributed to the use of cyclodextrins as excipients. Unlike the lactose-based carrier used in the commercial Onbrez® formulation, cyclodextrins act as surface-modifying agents, enabling fine-tuning of surface morphology and internal structure. This modification reduces interparticle cohesion, thereby enhancing the powders' flowability (M_{cas}) and dispersibility (C_{max}) during actuation, indicating that they aerosolized more rapidly and efficiently, releasing a greater mass of particles over a shorter exposure time compared to Onbrez®. Although DPI-SOL_{Crysmeb} exhibited tendentially higher C_{max} , M_{cas} and aerosolization yield, Fig. 7B and C show that no significant differences were observed in comparison to powder obtained from DPI-SUS_{HPβCD}.

Furthermore, the MMAD was evaluated for the two powders using a 9 stage Marple cascade impactor. Onbrez® resulted in having a statistically significant larger MMAD, illustrated in Fig. 8A, as compared to the IND/CIC developed powders from dried solutions and suspensions. Powders from atomized solutions (DPI-SOL_{Crysmeb}) and suspensions (DPI-SUS_{HPβCD}) exhibited comparable MMAD values, both below $5 \mu m$ and consistent with MMAD values previously obtained using the NGI. All the three test powders had an adequate GSD within the appropriate range for pharmaceutical heterodisperse aerosol (Bianco et al., 2021), between 1.5–2.5 (Fig. 8B).

During the PSD analysis, the aerosol particles travel through the PreciseInhale® system to the impactor after being aerosolized. In this process, losses can occur due to particle deposition on internal surfaces, particles bypassing the impactor stages, particle rebound, or inefficiencies in the collection system (Lexmond et al., 2018; Thakur et al., 2022). Therefore, the aerosol collection efficiency was calculated as the recovery. The recovery, represented on Fig. 9A, measures the amount of the aerosolized material captured on the stages of the Marple Cascade Impactor. As for the yield, both engineered powders exhibited comparable recovery rates, both of which were significantly higher than that of Onbrez® ($p < 0.0001$).

Alongside MMAD, the FPF is one of the most common descriptors for the aerosol deposition properties of DPI formulations (Xu et al., 2022). All three powders exhibited a relatively high FPF, exceeding 60 % (Fig. 9B), likely attributable to their favorable inhalation properties and appropriate flow rates. However, Onbrez® displayed a lower FPF compared to developed powders from dried solution and suspension. In contrast, powder from atomized solution also exhibited a significantly higher FPF than powders from dried suspensions, which is partly attributable to its slightly smaller MMAD. As for the aerosolization

properties, developed engineered powders in this study showed a more favorable lung deposition profile than Onbrez®, due to higher FPF and lower MMAD.

Overall, the PreciseInhale® system is an advanced aerosol generation system which enables precision dosing of powders' aerosol and is widely used in *in vivo*, *ex vivo*, and *in vitro* studies to investigate the solubility, dissolution, and pharmacokinetic/pharmacodynamic profiles of airborne particles (Eedara et al., 2022; Sciuscio et al., 2019). While its application in these contexts is well established, its potential for characterizing aerosolization properties of powders, particularly in comparison with the NGI, remains less explored.

In this study, the aerosol performance of DPI powders was evaluated using both the NGI and PreciseInhale® systems, demonstrating the complementarity between these two techniques. The NGI, a cascade impactor that operates at constant flow rates, provides detailed aerodynamic particle size distribution. On the other hand, the PreciseInhale® system primarily functions as an aerosol generation and delivery device, offering precise control over flow rate, aerosol volume, and generation duration. This precision allows the system to closely replicate human inhalation dynamics, making it a valuable tool for translational respiratory research and preclinical inhalation studies. When combined with a Marple Cascade Impactor, it facilitates a thorough analysis of aerosolization and deposition profiles, along with real-time monitoring of aerosol concentration during dispersion. The integration of this system allows for the collection of additional performance metrics (such as C_{max} , M_{cas} , and yield) that offer novel insights into powder dispersibility, flowability, and aerosol delivery efficiency, metrics that are not typically captured by NGI analysis alone, while still confirming the aerodynamic properties of the powders.

Indeed, despite differences in methodology, both systems revealed consistent trends in aerosolization performance. Specifically, atomized solutions (DPI-SOL_{Crysmeb}) outperformed dried suspensions (DPI-SUS_{HPβCD}) in both systems, demonstrating higher FPF values and lower MMAD. The commercial Onbrez® formulation consistently exhibited the lowest performance, likely due to its larger particle size and sub-optimal excipient morphology.

In this context, the integration of NGI and PreciseInhale® data offers a more comprehensive evaluation of inhalation powders, combining aerodynamic size profiling with aerosol delivery dynamics. While NGI remains the gold standard for aerodynamic characterization, PreciseInhale® complements this by providing additional parameters related to aerosolization behavior and lung deposition potential. Together, these *in vitro* approaches offer novel insights into powder dispersibility, flowability, and aerosol delivery efficiency, deepening the understanding of inhalation product performance and supporting the

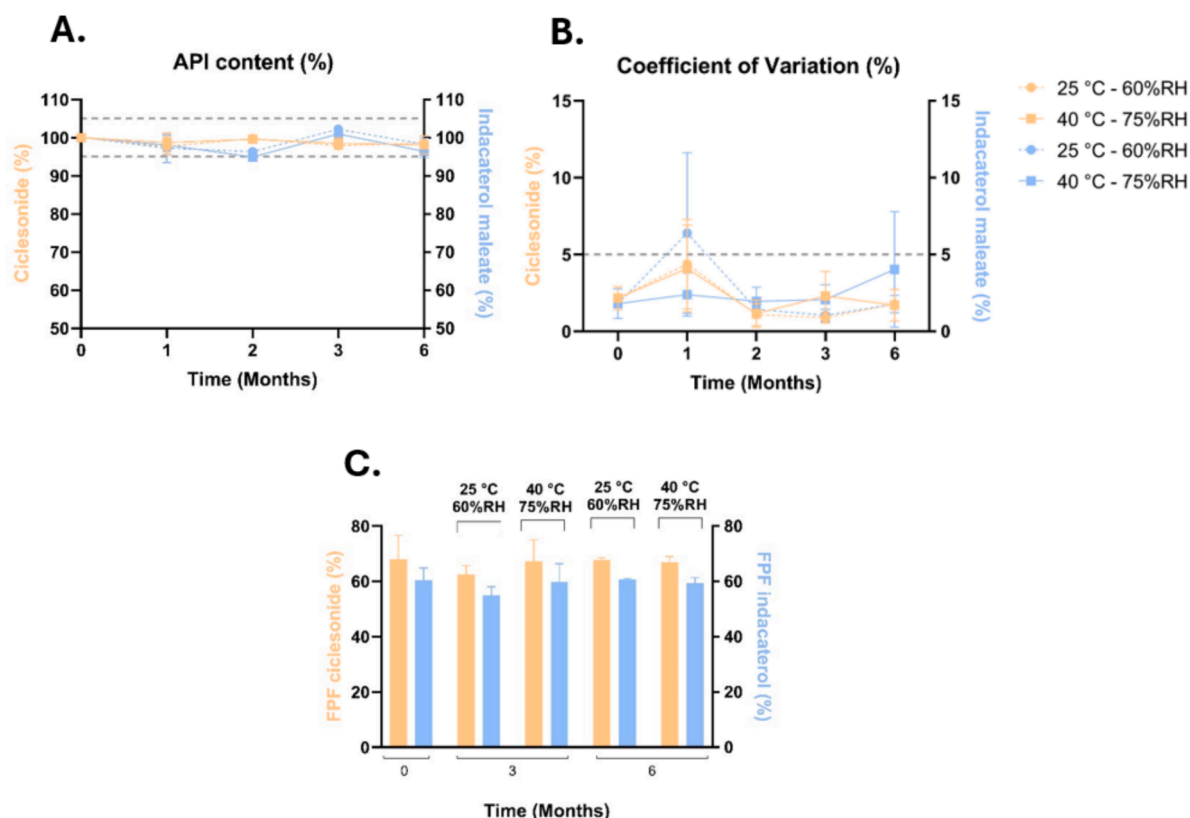


Fig. 10. (A) CIC and IND content from powders from atomized solutions (DPI-SOL_{Crysmeb}) with 10 % solid content (w/v), monitored over six months under ICH stability conditions. (B) Coefficients of variation for APIs across five samples produced from powders from atomized solutions with 10 % solid content (w/v), monitored over six months under ICH stability conditions. (C) CIC and IND FPF values from powders from atomized solutions with 10 % solid content (w/v), monitored over six months under ICH stability conditions. Analyses were performed in triplicates (n = 3) and results are presented as mean \pm standard deviation.

optimization of formulations prior to *in vivo* studies. Ultimately, this combination of complementary techniques enhances the reliability of performance trends and establishes a robust foundation for selecting and optimizing formulations for further development.

3.5. Powders stability

While many studies suggest that dry formulations improve stability (Chrystyn et al., 2023), others highlight the potential instability of SD powders, primarily due to high humidity sensitivity and to their hygroscopic properties (Radivojev et al., 2019; Shetty et al., 2020). Given these concerns, a stability study was conducted on the most promising formulation. Among the powders developed, those produced from atomized solutions (10 % solid content), DPI-SOL_{Crysmeb}, demonstrated significantly enhanced aerodynamic properties and aerosolization efficiency, highlighting their strong potential for inhalation applications.

Regarding the physicochemical properties over time, the powder's particle size remained unchanged after 6 months under both tested conditions. Powder's moisture content, which is around 6 % for both storage conditions, remained stable after 6 months (Supplementary data F A). A small increase in water content may lead to slight agglomeration of the powder (Supplementary data F B). Monitoring the moisture content over time is crucial to ensure proper aerosolization and aerodynamic performance while preventing potential API degradation and maintaining the therapeutic efficacy of the powder (Abiona et al., 2022;

Shetty et al., 2020). To minimize moisture uptake for further investigation of this developed powder, solutions such as incorporating desiccant tablets or optimizing the packaging with moisture-resistant materials can be considered.

About the API content in powders over time results, presented in Fig. 10A, show that both active substance contents were not impacted over time, whatever the temperature or RH tested, because API content remained between 95 and 105 % of the initial content. Furthermore, Fig. 10B shows that the optimized powder from the atomized solution maintained API homogeneity after 6 months under both ICH conditions, suggesting that the slight moisture increase did not cause agglomeration. Finally, *in vitro* aerodynamics profiles after 3 and 6 months remained similar for both API, at both conservation characteristics, and this is proven by identical and FPF results for both active substances, as shown by Fig. 10C, with similar MMAD and GSD values. This stability is further enhanced by the use of non-reducing sugars, specifically cyclodextrin Crysmeb in the optimized powder, which exhibit higher T_g, leading to improved API stability due to their amorphous state at room temperature (Lechanteur and Evrard, 2020). This underscores the critical importance of excipient selection in the production of DPIs.

4. Conclusion

Limited lung deposition reduces the efficacy of many commercial inhalation powders. Addressing this requires improved formulation

strategies, better understanding of inhalation dynamics, exploration of new API combinations, and enhanced evaluation methods to develop more effective treatments for pulmonary diseases.

To address this, in this study, a successful combination developed a dry powder inhaler combining ciclesonide and indacaterol maleate for asthma and COPD treatment. Optimized spray-dried powders from atomized solutions demonstrated superior aerosolization, lung deposition, and physicochemical properties compared to those from suspensions. The solubilization of APIs in the atomized liquid, facilitated by cyclodextrin excipients, played a key role in obtaining favorable particle size, recovery, and stability in multi-API formulations.

Additionally, consistent and complementary results obtained from both the Next-Generation Impactor (NGI) and the PreciseInhale® system validated the *in vitro* aerosolization performance of the developed formulation, reinforcing the reliability of the findings. This strong agreement highlights the potential of the new carrier-free DPI to enhance therapeutic efficacy across a range of patient profiles. However, evaluating the *in vivo* performance of inhaled powders remains a significant challenge (Price et al., 2019). Bridging this gap calls for novel *in vitro* methods and advanced equipment capable of better predicting *in vivo* outcomes. These findings lay a solid foundation for future *in vivo* studies and the continued development of optimized inhalable therapies for respiratory diseases.

CRedit authorship contribution statement.

Laure-Anne Bya: Writing – original draft, Writing – review & editing, Investigation, Data curation, Conceptualization. **Benedetta Bottero:** Conceptualization, Writing – review & editing, Investigation, Data curation. **Alice Coeurderoi:** Data curation. **T. Nghia Dinh:** Review. **Pierre-Yves Sacré:** Data curation. **Eric Ziemons:** Data curation. **Géraldine Piel:** Supervision. **Didier Cataldo:** Supervision. **Brigitte Evrard:** Supervision. **Anna Lechanteur:** Supervision, Writing – review & editing.

CRedit authorship contribution statement

L.-A. Bya: Writing – review & editing, Writing – original draft, Investigation, Data curation, Conceptualization. **B. Bottero:** Writing – review & editing, Investigation, Data curation, Conceptualization. **A. Coeurderoi:** Data curation. **T. Nghia Dinh:** Supervision. **P.Y. Sacré:** Data curation. **E. Ziemons:** Data curation. **D. Cataldo:** Supervision. **G. Piel:** Supervision. **B. Evrard:** Supervision. **A. Lechanteur:** Writing – review & editing, Supervision.

Declaration of competing interest

The authors declare that they have no known competing financial interests or personal relationships that could have appeared to influence the work reported in this paper.

Acknowledgement

This research was funded by the Walloon Region, SPW-EER, DGO6 – Win2Wal – LNPulmo convention n°2210043 and supported by the Léon Fredericq Foundation. Authors want to thank Aquilon Pharma (Liège, Belgium). Authors want to thank Dr. Erwan Plougonven from the PEPs (Prof. Angélique Léonard – University of Liege, Belgium) for the scanning electron microscopy analysis.

Appendix A. Supplementary data

Supplementary data to this article can be found online at <https://doi.org/10.1016/j.ijpharm.2025.125696>.

Data availability

No data was used for the research described in the article.

References

- Abadelah, M., Chrystyn, H., Bagherisadeghi, G., Abdalla, G., Larhrib, H., 2018. Study of the emitted dose after two separate inhalations at different inhalation flow rates and volumes and an assessment of aerodynamic characteristics of inhaled Ondre Breezhale® 150 and 300 µg. *AAPS PharmSciTech* 19, 251–261. <https://doi.org/10.1208/s12249-017-0841-y>.
- Abiona, O., Wyatt, D., Koner, J., Mohammed, A., 2022. The optimisation of carrier selection in dry powder inhaler formulation and the role of surface energetics. *Biomedicines* 10, 2707. <https://doi.org/10.3390/biomedicines10112707>.
- Aiassa, V., Garnerio, C., Zoppi, A., Longhi, M.R., 2023. Cyclodextrins and their derivatives as drug stability modifiers. *Pharmaceuticals*. <https://doi.org/10.3390/ph16081074>.
- Azouz, W., Chetcuti, P., Hosker, H.S.R., Saralaya, D., Stephenson, J., Chrystyn, H., 2015. The inhalation characteristics of patients when they use different dry powder inhalers. *J Aerosol Med Pulm Drug Deliv* 28, 35–42. <https://doi.org/10.1089/jamp.2013.1119>.
- Baloira, O., Abad, A., Fuster, A., Rivero, J.L.G., García-Sidro, P., Márquez-Martín, E., Palop, M., Soler, N., Velasco, J.L., González-Torralba, F., 2021. Lung deposition and inspiratory flow rate in patients with chronic obstructive pulmonary disease using different inhalation devices: A systematic literature review and expert opinion. *Int J Chron Obstruct Pulmon Dis*. <https://doi.org/10.2147/COPD.S297980>.
- Barnes, P.J., 2017. Cellular and molecular mechanisms of asthma and COPD. *Clin Sci*. <https://doi.org/10.1042/CS20160487>.
- Behboudi-Jobbehdar, S., Soukoulis, C., Yonekura, L., Fisk, I., 2013. Optimization of Spray-Drying Process Conditions for the Production of Maximally Viable Microencapsulated L. acidophilus NCIMB 701748. *Dry Technol* 31, 1274–1283. <https://doi.org/10.1080/07373937.2013.788509>.
- Bianco, F., Salomone, F., Milesi, I., Murgia, X., Bonelli, S., Pasini, E., Dellacà, R., Ventura, M.L., Pillow, J., 2021. Aerosol drug delivery to spontaneously-breathing preterm neonates: lessons learned. *Respir Res*. <https://doi.org/10.1186/s12931-020-01585-9>.
- Cataldo, D., Corhay, J.L., Derom, E., Louis, R., Marchand, E., Michils, A., Ninane, V., Peché, R., Pilette, C., Vincken, W., Janssens, W., 2017. A belgian survey on the diagnosis of asthma– COPD overlap syndrome. *Int J Chron Obstruct Pulmon Dis* 12, 601–613. <https://doi.org/10.2147/COPD.S124459>.
- Chang, R.Y.K., Chan, H.K., 2022. Advancements in Particle Engineering for Inhalation Delivery of Small Molecules and Biotherapeutics. *Pharm Res*. <https://doi.org/10.1007/s10955-022-03363-2>.
- Chaurasiya, B., Zhao, Y.Y., 2021. Dry powder for pulmonary delivery: A comprehensive review. *Pharmaceutics*. <https://doi.org/10.3390/pharmaceutics13010031>.
- Takeda Canada Inc., 2012. PRODUCT MONOGRAPH Alvesco®. URL www.takedacanada.com.
- Chew, N.Y.K., Chan, H.-K., 2001. Use of Solid Corrugated Particles to Enhance Powder Aerosol Performance.
- Chow, M.Y.T., Kwok, P.C.L., Yang, R., Chan, H.K., 2020. Predicting the composition and size distribution of dry particles for aerosols and sprays of suspension: A Monte Carlo approach. *Int J Pharm* 582. <https://doi.org/10.1016/j.ijpharm.2020.119311>.
- Chrystyn, H., Azouz, W., Tarsin, W., 2023. Dry Powder Inhalers: From Bench to Bedside. *J Aerosol Med Pulm Drug Deliv* 36, 324–335. <https://doi.org/10.1089/jamp.2023.29103.hc>.
- Dal Negro, R.W., 2015. Dry powder inhalers and the right things to remember: A concept review. *Multidiscip Respir Med*. <https://doi.org/10.1186/s40248-015-0012-5>.
- Darquenne, C., 2020. Deposition Mechanisms. *J Aerosol Med Pulm Drug Deliv* 33, 181–185. <https://doi.org/10.1089/jamp.2020.29029.cd>.
- Das, S., Larson, I., Young, P., Stewart, P., 2009. Agglomerate properties and dispersibility changes of salmeterol xinafoate from powders for inhalation after storage at high relative humidity. *Eur J Pharm Sci* 37, 442–450. <https://doi.org/10.1016/j.ejps.2009.03.016>.
- de Boer, A.H., Hagedoorn, P., Hoppentocht, M., Buttini, F., Grasmeyer, F., Frijlink, H.W., 2017. Dry powder inhalation: past, present and future. *Expert Opin Drug Deliv*. <https://doi.org/10.1080/17425247.2016.1224846>.
- Deeks, E.D., Perry, C.M., Chapman, K., Chung, F., Brompton, R., NHS Trust, H., Mortimer, K., 2008. ADIS DRUG EVALUATION Ciclesonide A Review of its Use in the Management of Asthma, Drugs.
- Dufour, G., Bigazzi, W., Wong, N., Boschini, F., De Tullio, P., Piel, G., Cataldo, D., Evrard, B., 2015. Interest of cyclodextrins in spray-dried microparticles formulation for sustained pulmonary delivery of budesonide. *Int J Pharm* 495, 869–878. <https://doi.org/10.1016/j.ijpharm.2015.09.052>.
- Eedara, B.B., Bastola, R., Das, S.C., 2022. Dissolution and Absorption of Inhaled Drug Particles in the Lungs. *Pharmaceutics*. <https://doi.org/10.3390/pharmaceutics14122667>.
- Elsayed, M.M.A., Alfagih, I.M., Brockbank, K., Aodah, A.H., Ali, R., Almansour, K., Shalash, A.O., 2024. Critical attributes of fine excipient materials in carrier-based dry powder inhalation formulations: The particle shape and surface properties. *Int J Pharm* 655. <https://doi.org/10.1016/j.ijpharm.2024.123966>.
- Evrard, B., Bertholet, P., Gueders, M., Flament, M.P., Piel, G., Delattre, L., Gayot, A., Leterme, P., Foidart, J.M., Cataldo, D., 2004. Cyclodextrins as a potential carrier in drug nebulization. *Journal of Controlled Release* 96, 403–410. <https://doi.org/10.1016/j.jconrel.2004.02.010>.
- Ewing, P., Oag, S., Lundqvist, A., Stomilovic, S., Stellert, I., Antonsson, M., Nunes, S.F., Andersson, P.U., Tehler, U., Sjöberg, C., Péterffy, A., Gerde, P., 2021. Airway Epithelial Lining Fluid and Plasma Pharmacokinetics of Inhaled Fluticasone Propionate and Salmeterol Xinafoate in Mechanically Ventilated Pigs. *J Aerosol Med Pulm Drug Deliv* 34, 231–241. <https://doi.org/10.1089/jamp.2020.1637>.
- Fioni, A., Selg, E., Cenacchi, V., Acevedo, F., Brogini, G., Gerde, P., Puccini, P., 2018. Investigation of Lung Pharmacokinetic of the Novel PDE4 Inhibitor CHF6001 in

- Preclinical Models: Evaluation of the PreciseInhale Technology. *J Aerosol Med Pulm Drug Deliv* 31, 61–70. <https://doi.org/10.1089/jamp.2017.1369>.
- Geller, D.E., Weers, J., Heuerding, S., 2011. Development of an inhaled dry-powder formulation of tobramycin using pulmosphere™ technology. *J Aerosol Med Pulm Drug Deliv*. <https://doi.org/10.1089/jamp.2010.0855>.
- Gerde, P., Ewing, P., Låstbom, L., Ryrfeldt, Å., Waher, J., Lidén, G., 2004. A Novel Method to Aerosolize Powder for Short Inhalation Exposures at High Concentrations: Isolated Rat Lungs Exposed to Respirable Diesel Soot. *Inhal Toxicol* 16, 45–52. <https://doi.org/10.1080/08958370490258381>.
- Gerde, P., Nowenwik, M., Sjöberg, C.O., Selg, E., 2020. Adapting the Aerogen Mesh Nebulizer for Dried Aerosol Exposures Using the PreciseInhale Platform. *J Aerosol Med Pulm Drug Deliv* 33, 116–126. <https://doi.org/10.1089/jamp.2019.1554>.
- Gresse, E., Rousseau, J., Akdim, M., du Bois, A., Lechanteur, A., Evrard, B., 2024. Enhancement of inhaled micronized powder flow properties for accurate capsules filling. *Powder Technol* 437, 119576. <https://doi.org/10.1016/j.powtec.2024.119576>.
- Haidl, P., Heindl, S., Siemon, K., Bernacka, M., Cloes, R.M., 2016. Inhalation device requirements for patients' inhalation maneuvers. *Respir Med*. <https://doi.org/10.1016/j.rmed.2016.07.013>.
- Hebbink, G.A., Jaspers, M., Peters, H.J.W., Dickhoff, B.H.J., 2022. Recent developments in lactose blend formulations for carrier-based dry powder inhalation. *Adv Drug Deliv Rev*. <https://doi.org/10.1016/j.addr.2022.114527>.
- Horváth, A., Balász, L., Tomisa, G., Farkas, Á., 2017. Significance of breath-hold time in dry powder aerosol drug therapy of COPD patients. *Eur J Pharm Sci* 104, 145–149. <https://doi.org/10.1016/j.ejps.2017.03.047>.
- Hua, J., Ian, Ye, X., fen, Du, C., ling, Xie, N., Zhang, Jie qing, Li, M., Zhang, Jing, 2021. Optimizing inhalation therapy in the aspect of peak inhalation flow rate in patients with chronic obstructive pulmonary disease or asthma. *BMC Pulm Med* 21. DOI: 10.1186/s12890-021-01674-5.
- Karner, S., Anne Urbanetz, N., 2011. The impact of electrostatic charge in pharmaceutical powders with specific focus on inhalation-powders. *J Aerosol Sci*. <https://doi.org/10.1016/j.jaerosci.2011.02.010>.
- Khanal, D., Ke, W.R., Chan, H.K., 2022. Raman spectroscopic evaluation of crystallinity, chemical composition and stability of pharmaceutical powder aerosols. *Int J Pharm* 611. <https://doi.org/10.1016/j.ijpharm.2021.121341>.
- Lechanteur, A., Evrard, B., 2020. Influence of composition and spray-drying process parameters on carrier-free DPI properties and behaviors in the lung: A review. *Pharmaceutics* 12. <https://doi.org/10.3390/pharmaceutics12010055>.
- Lechanteur, A., Gresse, E., Orozco, L., Plougonven, E., Léonard, A., Vandewalle, N., Lumay, G., Evrard, B., 2023. Inhalation powder development without carrier: How to engineer ultra-flying microparticles? *Eur J Pharm Biopharm* 191, 26–35. <https://doi.org/10.1016/j.ejpb.2023.08.010>.
- Lechanteur, A., Plougonven, E., Orozco, L., Lumay, G., Vandewalle, N., Léonard, A., Evrard, B., 2022. Engineered-inhaled particles: Influence of carbohydrates excipients nature on powder properties and behavior. *Int J Pharm* 613. <https://doi.org/10.1016/j.ijpharm.2021.121319>.
- LeClair, D.A., Cranston, E.D., Xing, Z., Thompson, M.R., 2016. Optimization of Spray Drying Conditions for Yield, Particle Size and Biological Activity of Thermally Stable Viral Vectors. *Pharm Res* 33, 2763–2776. <https://doi.org/10.1007/s11095-016-2003-4>.
- Lexmond, A.J., Keir, S., Terakosolphan, W., Page, C.P., Forbes, B., 2018. A novel method for studying airway hyperresponsiveness in allergic Guinea pigs in vivo using the preciseinhaler system for delivery of dry powder aerosols. *Drug Deliv Transl Res* 8, 760–769. <https://doi.org/10.1007/s13346-018-0490-z>.
- Littringer, E.M., Mescher, A., Eckhard, S., Schröttner, H., Langes, C., Fries, M., Griesser, U., Walzel, P., Urbanetz, N.A., 2012. Spray drying of Mannitol as a drug carrier—the impact of process parameters on product properties. *Dry Technol* 30, 114–124. <https://doi.org/10.1080/07373937.2011.620726>.
- Magramane, S., Vlahović, K., Gordon, P., Kállai-Szabó, N., Zekő, R., Antal, I., Farkas, D., 2023. Inhalation Dosage Forms: A Focus on Dry Powder Inhalers and Their Advancements. *Pharmaceutics*. <https://doi.org/10.3390/ph16121658>.
- Malmjöf, M., Nowenwik, M., Meelich, K., Rådberg, I., Selg, E., Burns, J., Mascher, H., Gerde, P., 2019. Effect of particle deposition density of dry powders on the results produced by an in vitro test system simulating dissolution- and absorption rates in the lungs. *Eur J Pharm Biopharm* 139, 213–223. <https://doi.org/10.1016/j.ejpb.2019.03.005>.
- Marante, T., Viegas, C., Duarte, I., Macedo, A.S., Fonte, P., 2020. An overview on spray-drying of protein-loaded polymeric nanoparticles for dry powder inhalation. *Pharmaceutics* 12, 1–23. <https://doi.org/10.3390/pharmaceutics12111032>.
- Marianni, B., Polonini, H., Oliveira, M.A.L., 2021. Ensuring homogeneity in powder mixtures for pharmaceuticals and dietary supplements: Evaluation of a 3-axis mixing equipment. *Pharmaceutics* 13. <https://doi.org/10.3390/pharmaceutics13040563>.
- Matilainen, L., Toropainen, T., Vihola, H., Hirvonen, J., Järvinen, T., Jarho, P., Järvinen, K., 2008. In vitro toxicity and permeation of cyclodextrins in Calu-3 cells. *Journal of Controlled Release* 126, 10–16. <https://doi.org/10.1016/j.jconrel.2007.11.003>.
- Mitta, S.G., Tanvi, S., Bhargavi, U., Ruchitha, V., 2024. An Overview on Pulmonary Insulin. *Global Academic Journal of Pharmacy and Drug Research* 6, 12–19. <https://doi.org/10.36348/gajpdr.2024.v06i02.001>.
- Myers, T.R., 2013. The science guiding selection of an aerosol delivery device. *Respir Care* 58, 1963–1973. <https://doi.org/10.4187/respcare.02812>.
- Nave, R., Mcracken, N., 2008. Metabolism of ciclesonide in the upper and lower airways: review of available data. *Journal of Asthma and Allergy*.
- Negi, A., Nimbar, S., Moses, J.A., 2023. Engineering Inhalable Therapeutic Particles: Conventional and Emerging Approaches. *Pharmaceutics*. <https://doi.org/10.3390/pharmaceutics15122706>.
- Nguyen, D., Rasmuson, A., Björn, I.N., Thalberg, K., 2015. Mechanistic time scales in adhesive mixing investigated by dry particle sizing. *Eur J Pharm Biopharm* 69, 19–25. <https://doi.org/10.1016/j.ejps.2014.12.016>.
- Ou, C., Hang, J., Deng, Q., 2020. Particle deposition in human lung airways: Effects of airflow, particle size, and mechanisms. *Aerosol Air Qual Res* 20, 2846–2858. <https://doi.org/10.4209/aaqr.2020.02.0067>.
- Paudel, A., Worku, Z.A., Meeus, J., Guns, S., Van Den Mooter, G., 2013. Manufacturing of solid dispersions of poorly water soluble drugs by spray drying: Formulation and process considerations. *Int J Pharm*. <https://doi.org/10.1016/j.ijpharm.2012.07.015>.
- Price, D.N., Kunda, N.K., Muttill, P., 2019. Challenges associated with the pulmonary delivery of therapeutic dry powders for preclinical testing. *KONA Powder Part. J.* <https://doi.org/10.14356/kona.2019008>.
- Radiojevo, S., Pinto, J.T., Fröhlich, E., Paudel, A., 2019. Insights into DPI sensitivity to humidity: An integrated in-vitro-in-silico risk-assessment. *J Drug Deliv Sci Technol* 52, 803–817. <https://doi.org/10.1016/j.jddst.2019.05.047>.
- Rodrigo, G.J., Castro-Rodríguez, J.A., 2012. Safety of long-acting β agonists for the treatment of asthma: Clearing the air. *Thorax*. <https://doi.org/10.1136/thx.2010.155648>.
- Rossi, A., Polese, G., 2013. Indacaterol: A comprehensive review. *Int J Chron Obstruct Pulmon Dis*. <https://doi.org/10.2147/COPD.S21625>.
- Santos, P.S., Souza, L.K.M., Araujo, T.S.L., Medeiros, J.V.R., Nunes, S.C.C., Carvalho, R. A., Pais, A.C.C., Veiga, F.J.B., Nunes, L.C.C., Figueiras, A., 2017. Methyl- β -cyclodextrin inclusion complex with β caryophyllene: Preparation, characterization, and improvement of pharmacological activities. *ACS Omega* 2, 9080–9094. <https://doi.org/10.1021/acsomega.7b01438>.
- Saokham, P., Muankaew, C., Jansook, P., Loftsson, T., 2018. Solubility of cyclodextrins and drug/cyclodextrin complexes. *Molecules*. <https://doi.org/10.3390/molecules23051161>.
- Scherließ, R., Bock, S., Bungert, N., Neustock, A., Valentin, L., 2022. Particle engineering in dry powders for inhalation. *Eur J Pharm Sci* 172. <https://doi.org/10.1016/j.ejps.2022.106158>.
- Sciucio, D., Hoeng, J., Peitsch, M.C., Vanscheeuwijck, P., 2019. Respirable aerosol exposures of nicotine dry powder formulations to in vitro, ex vivo, and in vivo pre-clinical models demonstrate consistency of pharmacokinetic profiles. *Inhal Toxicol* 31, 248–257. <https://doi.org/10.1080/08958378.2019.1662526>.
- Selg, E., Ewing, P., Acevedo, F., Sjöberg, C.O., Ryrfeldt, Å., Gerde, P., 2013. Dry powder inhalation exposures of the endotracheally intubated rat lung, ex vivo and in vivo: The pulmonary pharmacokinetics of fluticasone furoate. *J Aerosol Med Pulm Drug Deliv* 26, 181–189. <https://doi.org/10.1089/jamp.2012.0971>.
- Shahin, H.I., Chabiani, L., 2023. A comprehensive overview of dry powder inhalers for pulmonary drug delivery: Challenges, advances, optimization techniques, and applications. *J Drug Deliv Sci Technol*. <https://doi.org/10.1016/j.jddst.2023.104553>.
- Shetty, N., Cipolla, D., Park, H., Zhou, Q.T., 2020. Physical stability of dry powder inhaler formulations. *Expert Opin Drug Deliv*. <https://doi.org/10.1080/17425247.2020.1702643>.
- Sollobub, K., Cal, K., 2010. Spray drying technique: II. Current applications in pharmaceutical technology. *J Pharm Sci*. <https://doi.org/10.1002/jps.21963>.
- Sosnik, A., Seremeta, K.P., 2015. Advantages and challenges of the spray-drying technology for the production of pure drug particles and drug-loaded polymeric carriers. *Adv Colloid Interface Sci*. <https://doi.org/10.1016/j.cis.2015.05.003>.
- Spahn, J.E., Zhang, F., Smyth, H.D.C., 2022. Mixing of dry powders for inhalation: A review. *Int J Pharm*. <https://doi.org/10.1016/j.ijpharm.2022.121736>.
- Sun, Y., 2016. Carrier free inhaled dry powder of budesonide tailored by supercritical fluid particle design. *Powder Technol* 304, 248–260. <https://doi.org/10.1016/j.powtec.2016.07.036>.
- Thakur, A., Xu, Y., Cano-Garcia, G., Feng, S., Rose, F., Gerde, P., Andersen, P., Christensen, D., Foged, C., 2022. Optimizing the design and dosing of dry powder inhaler formulations of the cationic liposome adjuvant CAF®01 for pulmonary immunization. *Front. Drug Deliv* 2. <https://doi.org/10.3389/fddv.2022.973599>.
- Truffin, D., Marchand, F., Chatelais, M., Chène, G., Saias, L., Herbst, F., Lipner, J., King, A.J., 2024. Impact of Methylated Cyclodextrin KLEPTOSE® CRYSMEB on Inflammatory Responses in Human In Vitro Models. *Int J Mol Sci* 25, 9748. <https://doi.org/10.3390/ijms25179748>.
- Vehring, R., 2008. Pharmaceutical particle engineering via spray drying. *Pharm Res*. <https://doi.org/10.1007/s11095-007-9475-1>.
- Vehring, R., Foss, W.R., Lechuga-Ballesteros, D., 2007. Particle formation in spray drying. *J Aerosol Sci* 38, 728–746. <https://doi.org/10.1016/j.jaerosci.2007.04.005>.
- Wang, B., Wang, L., Yang, Q., Zhang, Y., Qinglai, T., Yang, X., Xiao, Z., Lei, L., Li, S., 2024. Pulmonary inhalation for disease treatment: Basic research and clinical translations. *Mater Today Bio*. <https://doi.org/10.1016/j.mtbio.2024.100966>.
- Weers, J., 2022. Suboptimal Inspiratory Flow Rates With Passive Dry Powder Inhalers: Big Issue or Overstated Problem? *Front. Drug Deliv* 2. <https://doi.org/10.3389/fddv.2022.855234>.
- Weers, J., Tarara, T., 2014. The PulmoSphere™ platform for pulmonary drug delivery. *Ther Deliv*. <https://doi.org/10.4155/tde.14.3>.
- Wijnhoven, H.A.H., Kriegsman, D.M.W., Hesselink, A.E., Penninx, B.W.J.H., De Haan, M., 2001. Determinants of different dimensions of disease severity in asthma and COPD: Pulmonary function and health-related quality of life. *Chest* 119, 1034–1042. <https://doi.org/10.1378/chest.119.4.1034>.
- Wu, L., Miao, X., Shan, Z., Huang, Y., Li, L., Pan, X., Yao, Q., Li, G., Wu, C., 2014. Studies on the spray dried lactose as carrier for dry powder inhalation. *Asian J Pharm Sci* 9, 336–341. <https://doi.org/10.1016/j.ajps.2014.07.006>.
- Wu, W.D., Liu, W., Gengenbach, T., Woo, M.W., Selomulya, C., Chen, X.D., Weeks, M., 2014. Towards spray drying of high solids dairy liquid: Effects of feed solid content

- on particle structure and functionality. *J Food Eng* 123, 130–135. <https://doi.org/10.1016/j.jfoodeng.2013.05.013>.
- Xu, Y., Harinck, L., Lokras, A.G., Gerde, P., Selg, E., Sjöberg, C.O., Franzyk, H., Thakur, A., Foged, C., 2022. Leucine improves the aerosol performance of dry powder inhaler formulations of siRNA-loaded nanoparticles. *Int J Pharm* 621. <https://doi.org/10.1016/j.ijpharm.2022.121758>.
- Ziaee, A., Albadarin, A.B., Padrela, L., Femmer, T., O'Reilly, E., Walker, G., 2019. Spray drying of pharmaceuticals and biopharmaceuticals: Critical parameters and experimental process optimization approaches. *Eur J Pharm Sci*. <https://doi.org/10.1016/j.ejps.2018.10.026>.
- Zillen, D., Beugeling, M., Hinrichs, W.L.J., Frijlink, H.W., Grasmeijer, F., 2021. Natural and bioinspired excipients for dry powder inhalation formulations. *Curr. Opin. Colloid Interface Sci*. <https://doi.org/10.1016/j.cocis.2021.101497>.